Inertial Instability and Mesoscale Convective Systems. Part I: Linear Theory of Inertial Instability in Rotating Viscous Fluids

KERRY A. EMANUEL[1]

Massachusetts Institute of Technology, Cambridge 02139

(Manuscript received 16 May 1979, in final form 23 July 1979)

ABSTRACT

Observations of strong convective lines in middle latitudes indicate a close association of the lines with the presence of vertical shear of the large-scale horizontal wind. Under the premise that this shear is necessary to the maintenance of mesoscale circulations accompanying the lines, it is found that the susceptibility of the large-scale momentum, temperature and moisture fields to such circulations is related to the inertial stability of the flow. Part I contains a description of a variational solution of the linear equations governing two-dimensional perturbations in a bounded, fully viscous, adiabatic and Boussinesq rotating fluid with constant vertical and horizontal shears. The principal finding of this analysis is that the horizontal length scale of the most unstable normal mode is determined primarily by the depth of the unstable domain and the slope of isentropic surfaces rather than by the diffusive properties of the fluid. The effects of moisture and the conditions under which inertial circulations are likely to develop in the atmosphere are examined in Part II and compared with observations of mesoscale convective systems.

1. Introduction

An important development in the atmospheric sciences over the last two decades has been the realization that convective systems, as distinct from the individual convective element, depend crucially on the presence of much larger circulations which supply moisture to the convection and may also destabilize the convective environment. This conceptual development originated in the CISK theory of tropical cyclone development, as first presented by Charney and Eliassen (1964), and ultimately led to the first successful parameterizations of cumulus convection (e.g., Arakawa and Shubert, 1974). The understanding and prediction of midlatitude convective systems such as squall lines have not greatly benefitted from these ideas, however. Attempts to relate the development of severe, persistent convective systems to the dynamics of the large scale (as resolved, for example, by the current North American rawinsonde network) have not been entirely successful (e.g., Fritsch *et al.*, 1976), and the nature of the supportive circulations and their interaction with cumuli remain enigmatic.

Observations of intense, persistent convective lines in middle latitudes invariably indicate the presence of conditional instability and strong vertical shear of the large-scale horizontal wind. Emphasis has been placed on the role of the latter in organizing motion on the convective scale. Independent of this idea, it is the premise here that the intensity and persistence of organized convection are determined by the susceptibility of the synoptic-scale temperature, moisture and momentum fields to *mesoscale* circulations, with dimensions greater than those typical of pure convection but less than those resolvable by most operational observation networks. We assert that while conditional instability is necessary for any convection, its presence may not be sufficient to permit the development of mesoscale circulations which supply moisture to the convection. On the other hand, certain large-scale distributions of momentum and density may be unstable to mesoscale perturbations in a convectively unstable atmosphere. The degree of this mesoscale instability, together with the amount of buoyant energy available to the cumuli, determine the intensity of the convection. The conditional instability allows the convection to occur in the first place; the synoptic-scale environment facilitates the development of mesoscale circulations which in turn support the convection by providing moisture convergence and by destabilizing the local convective environment.

In order to assess the stability of the large-scale flow to mesoscale disturbances, it is necessary to

[1] Present affiliation: Cooperative Institute for Mesoscale Meteorological Studies, University of Oklahoma, Norman 73019.

0022-4928/79/122425-25$10.25

take into account several parameters normally neglected on the cumulus scale, such as the absolute vorticity of the flow. Analytic examination of mesoscale dynamics is hampered by the intractability of making simplifying assumptions on the basis of scale; the motion fields are too small to be considered inviscid and quasi-geostrophic, but too large to neglect rotation or horizontal gradients in the environment. Fortunately, many extratropical convective systems are organized in lines and hence the mesoscale flow, in these cases, may be considered to be two dimensional. In particular, precold frontal squall lines comprise an interesting class of convective systems on which to test the aforementioned premise as their organization on the mesoscale is apparently simple, and as they have received much attention in observational studies of intense convection. A primary finding of these studies is that the lines occur in an environment characterized by strong vertical shear and are more or less aligned with the shear.

The stability of baroclinic shear flow in a stably-stratified rotating fluid to two-dimensional perturbations whose axes are aligned with the shear is the subject of Part I. By examining in detail the structure of inertial circulations in viscous shear flow, as well as the conditions under which they might occur, we hope to ascertain whether such motions resemble those observed in association with squall lines.

2. Review of inertial stability theory

Two-dimensional circulations with axes parallel to the shear vector in rotating fluids may occur if the flow is inertially unstable, i.e., if there exists an unstable balance of pressure gradient and centrifugal (Coriolis) forces within the fluid. The first investigation of the physical mechanism of inertial instability was carried out by Rayleigh (1916), who derived the stability criterion for a homogeneous, incompressible and inviscid circular vortex flow. Later, Solberg (1933) extended Rayleigh's analysis to include the effect of baroclinity. The fundamental conclusion of these investigations is that circular vortex flow is stable to axisymmetric disturbances as long as the square of the angular momentum of the flow increases with radius along isentropic surfaces, otherwise it is unstable. Due to the symmetry of the disturbances in the circular vortex, this form of disturbance has also been called symmetric instability.

For the special case of inviscid, Boussinesq, baroclinic flow on an f plane with constant vertical shears and no horizontal shear and bounded above and below by rigid surfaces, Stone (1966) finds that inertial circulations begin as overturning motions which are very nearly in the plane of isentropic surfaces. The largest linear growth rates are associated with rolls of vanishing horizontal scale in the direction transverse to the shear, although the dependence of the growth rate on this wavelength is not great for small wavelengths. The linear theory for this special case indicates that instability sets in when the Richardson number (Ri) falls below unity. The expressions derived by Stone for the growth rate (ω_i) and the largest wavelength ($L_{\max}$) for which the flow is unstable are

$$\omega_i = f\left(\frac{1}{\mathrm{Ri}} - 1\right)^{1/2},$$

$$L_{\max} = 2\frac{\bar{U}_z H}{f}(1 - \mathrm{Ri})^{1/2},$$

where f is the Coriolis parameter, $\bar{U}_z$ the constant shear value and H the depth of the fluid. The Richardson number is defined

$$\mathrm{Ri} \equiv \frac{\dfrac{g}{\theta_0}\dfrac{\partial\theta}{\partial z}}{\bar{U}_z^2}.$$

The vanishing length scale of the most rapidly growing linear mode in the bounded inviscid system suggests that the length scale of inertial circulations in real baroclinic fluids is determined by the diffusive properties of the fluid. The addition of viscosity to the linear symmetric stability problem greatly complicates its solution as the resulting equations are of much higher order. McIntyre (1970) found that the inertial stability equations are singular with respect to the diffusion parameters; i.e., the nature of the solutions of the viscous system in the limit of vanishing diffusion differs from the solution of the inviscid system. McIntyre studied symmetric instability in an unbounded viscous baroclinic fluid and found that monotonically growing disturbances begin when

$$\frac{\bar{\eta}}{f}\,\mathrm{Ri} < \frac{(1+\sigma)^2}{4\sigma}$$

and oscillatory instability may occur when

$$\frac{\bar{\eta}}{f}\,\mathrm{Ri} < \frac{(1+3\sigma)^2}{8\sigma(1+\sigma)},$$

where σ is the Prandtl number, and $\bar{\eta}$ is the absolute vorticity about a vertical axis. When $(\bar{\eta}/f)$ Ri is greater than unity, the most rapidly growing mode is one which maximizes the destabilizing influence of diffusion while minimizing viscous dissipation. This length scale is $O(\nu^{1/2}f^{-1/4}\bar{U}_z^{-1/4})$. If, however, the Richardson number is classically subcritical, another mode with infinite length scale is permitted in the unbounded system. The growth rates of both modes are $O(f)$.

The diffusive singularity appears in the de-

pendence of the above expressions for the critical Richardson number on the Prandtl number, which can remain finite in the limit of vanishing diffusion. Noting that the critical Ri for monotonic instability has a minimum for $\sigma = 1$, it is apparent that unequal diffusion of heat and momentum is destabilizing.

Walton (1975) extended McIntyre's analysis to include the effects of rigid boundaries and small nonlinearity. Using a perturbation expansion in $T_0^{-1/6}$, where

$$T_0 \equiv \frac{f^2H^4}{\nu^2},$$

Walton finds that diffusion in the presence of boundaries lowers the critical Richardson number for both the monotonic and oscillatory instabilities, and that the wavelength of the most rapidly growing mode is a weak function of the diffusion coefficients when the latter are asymptotically small. The large-scale inviscid mode present in the unbounded system does not appear when boundaries are present since flow parallel to the boundaries is always stable.

The fully viscous, linear, non-hydrostatic inertial stability problem has been solved exactly by Kuo (1954) for the special case of a neutrally stratified fluid confined above and below by rigid, free-slip boundaries. Solutions were obtained for horizontally unbounded disturbances as well as for motions confined by two vertical free-slip walls. The possibility of oscillatory instability is not considered, although it is shown that amplifying oscillatory motions are not possible when the Prandtl number is unity. Kuo finds that the flow becomes unstable when a normalized vertical shear parameter exceeds a critical value dependent on the Taylor number (T_0). The unstable motions begin as overturning cells which slope upward over the denser fluid, and with wavelengths on the order of the depth of the fluid.

Yanai and Tokioka (1969) performed a numerical experiment in order to simulate meridional motions in an axially symmetric vortex. In this experiment, the nonlinear inviscid equations of motion are integrated in a domain bounded above and below by rigid boundaries. The results are in accord with the linear theory but the horizontal wavelength is limited by the numerical grid size. An integration is also performed in which the region of instability is restricted to a small area within the domain; in this case the unstable motions are very much confined within the unstable region.

As inertial instability draws kinetic energy from the large-scale vertical and/or horizontal shear, it must transport momentum downgradient, as has been shown by Stone (1972). In so doing, the inviscid instability has very little first-order effect on the available potential energy. Walton (1975) and Stone (1972) find, however, that the destruction of the large-scale vertical shear produces a secondary, thermally direct circulation which transports both heat and zonal momentum poleward. Presumably, there exists a conversion from zonal available potential to zonal kinetic energy in this secondary circulation.

The investigations of inertial stability conducted thus far (a summary of which is presented in Table 1) have dealt for the most part with inviscid fluids and flows with asymptotically small viscosity. The singularity of the viscous equations demands, in this case, that the diffusive effects be formulated completely so as to resolve the structure of inertial circulations. In Section 3, we proceed to derive solutions of the perturbation equations for a fully viscous baroclinic flow with constant stratification and shear.

3. The linear perturbation equations

We here examine the stability of a rotating, fully viscous, Boussinesq baroclinic fluid to two-dimensional displacements transverse to the shear. We take as an equilibrium flow a steady zonal current on an f plane. The zonal flow is characterized by constant vertical and lateral shears, i.e.,

$$\bar{U} = \bar{U}_z z + \bar{U}_y y,$$

in which $\bar{U}_z$ and $\bar{U}_y$ are constant values of the vertical and horizontal shears, respectively. Similarly, the equilibrium density distribution is taken to be of the form

$$\ln\bar{\rho} = \frac{\partial \ln\bar{\rho}}{\partial y} y + \frac{\partial \ln\bar{\rho}}{\partial z} z,$$

where the horizontal density gradient satisfies the condition of thermal wind balance

$$f\bar{U}_z = g \frac{\partial \ln\bar{\rho}}{\partial y},$$

where f is the Coriolis parameter and g the acceleration of gravity. The square of the Brunt-Väisälä frequency is defined for a Boussinesq fluid as

$$N^2 \equiv -g \frac{\partial \ln\bar{\rho}}{\partial z} = \text{constant}.$$

Using these relations, the density distribution may be written

$$g \ln\bar{\rho} = f\bar{U}_z y - N^2 z.$$

The stability of this balanced initial state is explored by determining the time dependence of small perturbations superposed on the equilibrium flow. The perturbations are taken to be two-dimensional, with axes along the shear (no zonal variation).

TABLE 1. Summary of inertial stability investigations.

	Linear or nonlinear	Equilibrium flow	Boundaries	Criterion for instability	Wavelength of maximum growth
Rayleigh (1916)	L	Homogeneous, incompressible and inviscid circular vortex	None	$\frac{\partial M^2}{\partial r} < 0$ $(M = r^2\omega)$	—
Solberg (1933)	L	Inviscid, Boussinesq circular vortex with constant vertical shear and static stability	None	$\left(\frac{\partial M^2}{\partial r}\right)_\theta < 0$	—
Kuo (1954)	L	Viscous nonhydrostatic zonal flow with constant shear and neutral stratification	Rigid free-slip boundaries at bottom and top	$\frac{\bar{U}_z}{\bar{\eta}}(1+\sigma) > F(T_0)$	$O(H)$
Stone (1966)	L	Inviscid hydrostatic Boussinesq zonal flow with constant shear and static stability	Rigid top and bottom	$1 - \frac{1}{Ri} - \frac{\bar{U}_y}{f} < 0$	0
McIntyre (1969)	L	Viscous hydrostatic Boussinesq zonal flow with constant shear and static stability	None	$Ri < \frac{(1+\sigma)^2}{4\sigma}$	∞ or $O(\nu^{1/2}f^{-1/4}\bar{U}_z^{-1/4})$
Yanai and Tokioka (1969)	NL (numerical integration)	Inviscid zonal flow	Rigid free-slip at top and bottom	—	—
Walton (1975)	NL (weakly)	Viscous hydrostatic Boussinesq zonal flow with constant shear and static stability	Rigid at top and bottom	$\frac{4\sigma}{(1+\sigma)^2} Ri < F(T_0)$	$O(T_0^{-1/6}\bar{U}_z f^{-1}H)$

Stone (1966) has shown that such perturbations have higher growth rates than those with axes slightly skewed with respect to the shear.

Denoting the perturbations by primes, the linearized adiabatic Boussinesq equations are

$$\left(\frac{\partial}{\partial t} - \nu\nabla^2\right)u' + v'\bar{U}_y + w'\bar{U}_z = fv', \tag{1}$$

$$\left(\frac{\partial}{\partial t} - \nu\nabla^2\right)v' = -\frac{1}{\rho_0}\frac{\partial p'}{\partial y} - fu', \tag{2}$$

$$\alpha\left(\frac{\partial}{\partial t} - \nu\nabla^2\right)w' = -\frac{1}{\rho_0}\frac{\partial p'}{\partial z} - \frac{\rho'}{\rho_0}g, \tag{3}$$

$$\left(\frac{\partial}{\partial t} - \kappa\nabla^2\right)\frac{\rho'}{\rho_0} + \frac{f\bar{U}_z}{g}v' - \frac{N^2}{g}w' = 0, \tag{4}$$

$$\frac{\partial v'}{\partial y} + \frac{\partial w'}{\partial z} = 0. \tag{5}$$

The coefficients of momentum and heat diffusion are ν and κ, respectively, and α is a tag set equal to zero or unity depending on whether the flow is considered hydrostatic or not (this will depend on the shear and the static stability, as discussed later).

The perturbation flow in the y-z plane may be described in terms of a streamfunction by virtue of the form of the continuity equation (5). Such a variable is here defined so that

$$v' \equiv -\frac{\partial\psi}{\partial z}, \quad w' \equiv \frac{\partial\psi}{\partial y}.$$

Using this notation, the three momentum equations and the heat equation may be combined to yield a single eighth-order equation for the streamfunction:

$$\left(\frac{\partial}{\partial t} - \kappa\nabla^2\right)\left(\frac{\partial}{\partial t} - \nu\nabla^2\right)^2\left(\alpha\frac{\partial^2}{\partial y^2} + \frac{\partial^2}{\partial z^2}\right)\psi = -\left(\frac{\partial}{\partial t} - \nu\nabla^2\right)\left(f\bar{U}_z\frac{\partial^2\psi}{\partial y\,\partial z} + N^2\frac{\partial^2\psi}{\partial y^2}\right) - \left(\frac{\partial}{\partial t} - \kappa\nabla^2\right)\left(f\bar{U}_z\frac{\partial^2\psi}{\partial y\,\partial z} + f\bar{\eta}\frac{\partial^2\psi}{\partial z^2}\right). \tag{6}$$

Here $\bar{\eta}$ is defined as the absolute vorticity of the flow:

$$\bar{\eta} \equiv f - \bar{U}_y.$$

If an exponential time dependence is assumed and boundary conditions on the streamfunction are specified, then the relationship among the stability parameters, which appear as constant coefficients of (6), are determined as characteristic values of the latter. The time dependence may enter as both growth (or decay) and as oscillation.

We will approach the problem here by representing the streamfunction as a Fourier series in y and t, and then finding that component wave which first exhibits positive growth as the base flow

is altered toward an unstable condition. Assuming that the time dependence is of the form $\exp(\omega t)$, we will determine the nature of those solutions characterizing the marginal state in which $\mathrm{Re}(\omega) = 0$. The motions may set in as "overstability" if $\mathrm{Im}(\omega) \neq 0$ when $\mathrm{Re}(\omega) = 0$.

In order to condense the analysis, the following simplified cases will be examined:

Case (i): Disturbances are hydrostatic ($\alpha = 0$) and horizontal diffusion is neglected ($\nabla^2 = \partial^2/\partial z^2$).

Case (ii): Disturbances are nonhydrostatic ($\alpha = 1$), the fluid is neutrally stratified ($N^2 = 0$) and horizontal diffusion is included ($\nabla^2 = \partial^2/\partial y^2 + \partial^2/\partial z^2$).

The case (ii) corresponds exactly to the problem considered by Kuo (1954) and is included here primarily as a check on the methods of solution. It should be noted that when the fluid is nonhydrostatic, the orientation of the rotation axis with respect to the gravitational vector becomes an important consideration. In the present analysis, we take the rotation axis to lie along the gravitational vector as in Kuo (1954). In Appendix C the effects of including the meridional component of rotation are considered.[2]

The degree to which both the hydrostatic assumption and the neglect of horizontal diffusion are valid depends on the ratio of the vertical to horizontal length scales, which ratio, according to the scaling arguments to be presented shortly, depends on the slope of the potential isotherms $f\bar{U}_z/N^2$. If this slope is small, then vertical accelerations and horizontal diffusion may be neglected.

a. Boundary conditions

The boundaries at the top and bottom of the domain are specified as rigid ($w = 0$) and perfectly conducting ($\rho' = 0$). Since we wish to specify a constant vertical shear in the base state, we must also require the boundaries to be no-slip and differentially rotating, with the bottom boundary stationary and the top boundary rotating at the local tangential velocity $\bar{U}_z H$. However, we will impose stress-free boundary conditions on the *perturbation* velocities as a matter of mathematical convenience, though one should keep in mind that this is physically artificial. These stress-free conditions may be written

$$\left(\frac{\partial \psi}{\partial y}, \frac{\partial^2 \psi}{\partial z^2}, \frac{\partial u'}{\partial z}, \rho'\right) = 0 \quad \text{at boundaries.}$$

Additionally, the perturbation equations for case (i) are solved for no-slip boundaries:

$$\left(\frac{\partial \psi}{\partial y}, \frac{\partial \psi}{\partial z}, u', \rho'\right) = 0 \quad \text{at boundaries.}$$

The perturbations are assumed to be periodic in the direction transverse to the shear.

b. Overstable oscillations

McIntyre (1970) and Walton (1975) consider the possibility of over-stable oscillations in an unbounded fluid and in a bounded flow with asymptotically small diffusion, respectively. For the unbounded case, (6) may be solved for the normal modes using the substitution

$$\psi = |\Psi| \exp[i(rz + ly) + \omega t]$$

with r and l real and ω complex. With this substitution, (6) reduces to a cubic equation in ω which admits three real or one real and two complex conjugate roots. In the case of asymptotically small diffusion (or small wavenumber in the unbounded case), it is found that oscillatory instability may set in when

$$\mathrm{Ri} < \frac{(1 + 3\sigma)^2}{8\sigma(1 + \sigma)},$$

with the oscillation frequency at the critical Richardson number given by

$$\omega^2 = f^2 \frac{(1 - \sigma)^2}{(1 + 3\sigma)(1 + \sigma)}.$$

Oscillatory instability is not possible when $\sigma = 1$, and occurs for critical Richardson numbers which, for a given Prandtl number, are always smaller than those corresponding to the non-oscillatory mode of instability.

Analogous criteria may be obtained in case (ii) for nonhydrostatic oscillatory instability in a fluid with neutral stratification. In the limiting case of asymptotically small diffusion, the critical shear and oscillation frequency may be found as functions of the Prandtl number and the ratio of horizontal to vertical wavenumbers, i.e.,

$$\frac{\bar{U}_z}{\bar{\eta}} = \frac{2\sigma}{(1 + 3\sigma)(-l/r)},$$

$$\omega^2 = \frac{1 - \sigma}{(1 + 3\sigma)(1 + (l/r)^2)}.$$

The lowest critical value of the shear occurs as $l/r \to -\infty$, in which case the oscillation frequency vanishes. In any event, oscillatory instability is only possible in this case when $\sigma < 1$. For non-oscillatory instability, the critical shear is

$$\frac{\bar{U}_z}{\bar{\eta}} = \frac{1}{(1 + \sigma)(-l/r)}.$$

[2] The author is grateful to a reviewer for pointing out the need to consider the direction of the rotation axis when the flow is nonhydrostatic.

Comparing the critical shears of both forms of instability, for a given ratio (l/r), it seems that the oscillatory mode is a distinct possibility in neutrally stratified flow when $\sigma < 1$. As most geophysical flows are nearly hydrostatic, however, the linear theory indicates that oscillatory instability is unlikely. In the following treatment, therefore, we will restrict our attention to the non-oscillatory form of instability.

c. Scaling

The time-independent form of (6) may be twice integrated (see Appendix A) to yield a sixth-order equation for the streamfunction. For case (i), this will be

$$-\nu^2\kappa \frac{\partial^6\psi}{\partial z^6} = f\bar{U}_z(\nu + \kappa)\frac{\partial^2\psi}{\partial y\partial z} + \nu N^2\frac{\partial^2\psi}{\partial y^2} + \kappa f\bar{\eta}\frac{\partial^2\psi}{\partial z^2}. \quad (7)$$

For case (ii), (6) reduces to

$$-\nu^2\kappa(\nabla^2)^3\psi = f\bar{U}_z(\nu + \kappa)\frac{\partial^2\psi}{\partial y\partial z} + \kappa f\bar{\eta}\frac{\partial^2\psi}{\partial z^2}. \quad (8)$$

By an appropriate choice of scaling, the number of independent parameters involved in either (7) or (8) may be reduced to two. Rather than choose a viscous length scale, however, we take the vertical scale to be H under the premise that for reasonable values of the diffusive parameters, the disturbances will seek length scales determined by the geometry of the domain. It will be seen later that this premise is eminently justified. We then choose a scale for the horizontal dimension y such that the number of independent parameters in each of (7) and (8) is reduced to two. The resulting equations, together with their scaling, are as follows:

Case (i)

$$-\mathrm{T}\frac{\partial^6\psi}{\partial z^6} = \chi_i\frac{\partial^2\psi}{\partial y\partial z} + \chi_i\frac{\partial^2\psi}{\partial y^2} + \frac{\partial^2\psi}{\partial z^2},$$

$$z^* \to zH, \quad y^* \to yH\frac{N^2\sigma}{f\bar{U}_z(1+\sigma)}. \quad (9)$$

Case (ii)

$$-\mathrm{T}(\nabla^2)^3\psi = \chi_{ii}\frac{\partial^2\psi}{\partial y\partial z} + \frac{\partial^2\psi}{\partial z^2},$$

$$z^* \to zH, \quad y^* \to yH.$$

The asterisks denote dimensional variables. The nondimensional parameters that appear in (9) and (10) are

$$\mathrm{T} \equiv \frac{f}{\bar{\eta}}\frac{\nu^2}{f^2H^4} \text{ (a modified inverse Taylor number)},$$

$$\chi_i \equiv \frac{f}{\bar{\eta}}\frac{1}{\mathrm{Ri}}\frac{(1+\sigma)^2}{\sigma},$$

$$\chi_{ii} \equiv \frac{\bar{U}_z}{\bar{\eta}}(1+\sigma),$$

where

$$\sigma \equiv \nu/\kappa \quad \text{(Prandtl number)},$$

$$\mathrm{Ri} \equiv N^2/\bar{U}_z^2 \quad \text{(Richardson number)}.$$

The parameter χ in each case is a measure of the inertial instability of the flow, with instability favored by small static stability, large shear and small absolute vorticity. Instability is also favored by Prandtl numbers far from unity in case (i), and greater than unity in case (ii). T is a measure of the damping due to viscosity.

Though the perturbation equations will not be solved for the linear growth rate of the instabilities, it is important to know something about the order of magnitude of the growth rate. In the inviscid formulation, the inertial growth rate is $O(f)$, as shown, for example, by Stone (1966). When diffusion is added, a diffusive time scale must be considered as well, particularly in the case where diffusion makes the instability possible. As McIntyre (1970) has shown, however, both the inviscid and diffusive modes of instability have growth rates of $O(f^{1/2}\bar{U}_z^{1/2})$; physically the instability is fundamentally inertial in character, since the diffusion, when it is destabilizing, only acts to break the constraints of heat and/or angular momentum conservation following the parcel motions. The modes of instability considered here are extensions of the modes McIntyre considered in the unbounded formulation to the case where boundaries are considered, and may thus be taken to have growth rates of the same order.

The solution of (9) and (10) with boundary conditions specified, will yield the critical values of the parameters χ in each case, as functions of the viscous parameter T. Solutions of these characteristic value equations will also yield eigenfunctions ψ characterizing the onset of unstable motions.

d. Asymptotic behavior

As (9) and (10) are singular in the small parameter T, we cannot be sure that their eigenvalues and eigenfunctions approach the inviscid limit as T is made very small. Walton (1975) is able to show that for small T, the horizontal and vertical scales both vary as $\mathrm{T}^{1/6}$ and that the solutions do approach the inviscid limit uniformly. Taking T = 0 in (9) and applying the rigid boundary conditions $\psi = 0$ at $z = 0, 1$, the normal mode solution for case (i) is obtained immediately. The streamfunction ψ satisfies

$$\psi = \sin l\left(y - \frac{\chi_i}{2}z\right)\sin(n\pi z), \quad n = 1, 2, 3\ldots, \quad (11)$$

while χ_i must satisfy the eigenvalue equation

$$\frac{\chi_i^2}{4} - \chi_i = \frac{n^2\pi^2}{l^2},$$

where l is the horizontal wavenumber. The smallest value of χ_i is 4 and occurs as $l \to \infty$ corresponding to the results of Walton (1975). The disturbances slope upward over the denser fluid with a dimensionless slope of ½ when $\chi_i = 4$. Dimensionally, the slope of the disturbances is

$$\frac{\partial z}{\partial y} = \frac{f\bar{U}_z}{N^2}\left(\frac{1+\sigma}{2\sigma}\right).$$

This slope is greater than or less than that of the isentropic surfaces depending on whether the Prandtl number is less than or greater than unity. The minimum slope is half that of the isentropic surfaces when $\sigma \to \infty$; as the dimensional slope becomes large the hydrostatic assumption will no longer be valid.

The inviscid solution for case (ii) with the same boundary conditions is

$$\psi = \sin(n\pi z)\sin l(\tfrac{1}{2}\chi_{ii} z - y),$$

while the eigenvalue χ_{ii} satisfies

$$\chi_{ii} = 2\pi/l = L,$$

where L is the nondimensional wavelength. The minimum value of χ_{ii} is zero corresponding to a vanishing wavelength and a vertical disturbance orientation.

The primary conclusions to be drawn on the basis of the solution in the limit of no viscosity are that instability sets in when the product of the absolute vorticity and the Richardson number is of order unity (provided that the Prandtl number does not differ greatly from unity), and that the resulting disturbances consist of overturning motions along isentropic surfaces, with axes along the shear.

As the viscous parameter T becomes asymptotically large, we would expect that the critical value of the shear (χ) will also become large; a simple inspection of (9) and (10) would suggest that the term $\partial^2\psi/\partial z^2$ may be neglected in either case. These equations then become, respectively,

$$-\frac{\mathrm{T}}{\chi_i}\frac{\partial^6\psi}{\partial z^6} = \frac{\partial^2\psi}{\partial y\partial z} + \frac{\partial^2\psi}{\partial y^2} \quad (\mathrm{T}\to\infty),$$

$$-\frac{\mathrm{T}}{\chi_i}(\nabla^2)^3\psi = \frac{\partial^2\psi}{\partial y\partial z} \quad (\mathrm{T}\to\infty).$$

As both of the above contain only a single characteristic value T/χ, χ will be a linear function of T when the latter is large. This asymptotic behavior is indeed evident in the complete solutions.

4. Solution of the characteristic value equations by variational methods[3]

A general technique for solving linear eigenvalue problems, first developed by Pellew and Southwell (1940) and used extensively by Chandrasekhar (1961), will be applied to the solution of (10), with free-slip boundary conditions, and (9) with both free-slip and no-slip conditions. The reader is referred to Chandrasekhar's text for a discussion of the physical implications of the variational theorems.

a. Free-slip boundaries

As (9) is sixth-order in z, three boundary conditions are required at each of the upper and lower boundaries (a fourth condition has been used in reducing (6) to sixth-order). Two of these are

$$\partial\psi/\partial y = \partial^2\psi/\partial z^2 = 0, \quad \text{at} \quad z = 0, 1,$$

and follow directly from the statement of the boundary conditions. If (2) is differentiated once in z, it is evident that $\partial^4\psi/\partial z^4$ must also vanish at the boundaries, since $\partial u/\partial z = \partial p/\partial z = 0$ at $z = 0, 1$. The conditions applied to the solution of (9) therefore will be

$$\psi = \frac{\partial^2\psi}{\partial z^2} = \frac{\partial^4\psi}{\partial z^4} = 0, \quad \text{at} \quad z = 0, 1. \tag{12}$$

Suppose that χ is specified in (9). Then associated with a function ψ_j satisfying this equation will be a characteristic value T_j, i.e.,

$$\mathrm{T}_j\frac{\partial^6\psi_j}{\partial z^6} = -\chi\frac{\partial^2\psi_j}{\partial y\partial z} - \chi\frac{\partial^2\psi_j}{\partial y^2} - \frac{\partial^2\psi_j}{\partial z^2}.$$

If the above is multiplied through by a different solution ψ_i (corresponding to a characteristic value T_i) and the resulting equation is integrated between the boundaries in z and across one wavelength in y, then

$$\int_0^1\int_0^L \mathrm{T}_j\psi_i\frac{\partial^6\psi_j}{\partial z^6}\,dydz = -\chi\int_0^1\int_0^L \psi_i\frac{\partial^2\psi_j}{\partial y\partial z}\,dydz - \chi\int_0^1\int_0^L \psi_i\frac{\partial^2\psi_j}{\partial y^2}\,dydz - \int_0^1\int_0^L \psi_i\frac{\partial^2\psi_j}{\partial z^2}\,dydz,$$

where L is the dimensionless horizontal wavelength. (Henceforth, the domain of integration is assumed to be in the y-z plane.)

Applying the conditions (12) and a sequence of in-

[3] The reader uninterested in the methods of solution presented herein may proceed without loss of continuity to Section 5.

tegrations by parts, the preceding becomes

$$T_j \int_0^1 \int_0^L \frac{\partial^3\psi_i}{\partial z^3}\frac{\partial^3\psi_j}{\partial z^3} = \chi \int_0^1 \int_0^L \psi_i \frac{\partial^2\psi_j}{\partial y\,\partial z} - \chi \int_0^1 \int_0^L \frac{\partial\psi_i}{\partial y}\frac{\partial\psi_j}{\partial y} - \int_0^1 \int_0^L \frac{\partial\psi_i}{\partial z}\frac{\partial\psi_j}{\partial z}. \quad (13)$$

Using integration by parts, it may also be shown that

$$\int_0^1 \int_0^L \psi_i \frac{\partial^2\psi_j}{\partial y\,\partial z} = \int_0^1 \int_0^L \psi_j \frac{\partial^2\psi_i}{\partial y\,\partial z}.$$

With this symmetry, a switch in indices i and j in (13) indicates that

$$\int_0^1 \int_0^L \frac{\partial^3\psi_i}{\partial z^3}\frac{\partial^3\psi_j}{\partial z^3} = \delta_{ij},$$

where δ_{ij} is the Kronecker delta. The functions $\partial^3\psi_j/\partial z^3$ are therefore orthogonal and (13) may be written in the form

$$T = \frac{\chi \int_0^1 \int_0^L \psi \frac{\partial^2\psi}{\partial y\,\partial z} - \chi \int_0^1 \int_0^L \left(\frac{\partial\psi}{\partial y}\right)^2 - \int_0^1 \int_0^L \left(\frac{\partial\psi}{\partial z}\right)^2}{\int_0^1 \int_0^L \left(\frac{\partial^3\psi}{\partial z^3}\right)^2} \equiv \frac{I_1}{I_2}. \quad (14)$$

It may now be shown that *the function ψ which satisfies the boundary conditions (12) and maximizes the value of T as expressed by (14) is also a solution of the partial differential equation (9).* The proof of this theorem is given in Appendix B. By parallel arguments, one can show that for the non-hydrostatic case, (10) is satisfied if the value T expressed as

$$T = \frac{\chi_{ii} \int_0^1 \int_0^L \psi \frac{\partial^2\psi}{\partial y\,\partial z} - \int_0^1 \int_0^L \left(\frac{\partial\psi}{\partial z}\right)^2}{\int_0^1 \int_0^L \left[\left(\frac{\partial^3\psi}{\partial y^3}\right)^2 + 3\left(\frac{\partial^3\psi}{\partial y^2\partial z}\right)^2 + 3\left(\frac{\partial^3\psi}{\partial y\,\partial z^2}\right)^2 + \left(\frac{\partial^3\psi}{\partial z^3}\right)^2\right]} \quad (15)$$

is maximized with respect to a function ψ which also satisfies the boundary conditions (12).

In order to utilize the variational approach in the solution of (9) and (10), it is necessary to find functions ψ which maximize T in (14) for case (i) and (15) for case (ii). The orthogonality of the functions ψ suggests that we may expand ψ in a series of orthogonal functions, and for simplicity, we may require that each individual term in the expansion satisfies the conditions (12). In this case, the complete Fourier series

$$\psi = \sum_{n=1}^{\infty} \sin n\pi z (a_n \sin ly + b_n \cos ly) \quad (16)$$

meets these requirements.

For a specified horizontal wavenumber l, the Fourier coefficients a_n and b_n may be regarded as the variational parameters and the problem becomes one of finding those sets of a_n and b_n which maximize T in (14) or (15). By finding the characteristic value T for various wavenumbers l we may find that wavenumber which is associated with the highest value of T; this wavenumber presumably characterizes the onset of instability.

When T is expressed as in (14), i.e., $T = I_1/I_2$, the maximization of T with respect to each of the Fourier coefficients a_n and b_n yields the requirements that

$$\left.\begin{aligned} \frac{\partial I_1}{\partial a_n} - T\frac{\partial I_2}{\partial a_n} &= 0 \\ \frac{\partial I_2}{\partial b_n} - T\frac{\partial I_2}{\partial b_n} &= 0 \end{aligned}\right\}, \quad n = 1, 2, 3 \ldots. \quad (17)$$

The series (16) is substituted into the integral relation (14), the integrals are performed, and we proceed to maximize T with respect to the a_n's and b_n's using (17). When the series (16) is truncated to N terms, these operations yield two sets of N linear algebraic equations:

$$\left.\begin{aligned} -\chi_i \sum_{m=1}^{N} \left(\frac{4nm\pi}{m^2-n^2}\right)\epsilon_{nm} b_m + \left(\frac{1}{2}L\pi^2 n^2 + \frac{2\pi^2}{L}\chi_i + \frac{1}{2}L\pi^6 n^6 T\right)a_n &= 0 \\ \chi_i \sum_{m=1}^{N} \left(\frac{4nm\pi}{m^2-n^2}\right)\epsilon_{nm} a_m + \left(\frac{1}{2}L\pi^2 n^2 + \frac{2\pi^2}{L}\chi_i + \frac{1}{2}L\pi^6 n^6 T\right)b_n &= 0 \end{aligned}\right\}, \quad n = 1, 2, 3, \ldots, N. \quad (18)$$

Here ϵ_{nm} is defined

$$\epsilon_{nm} \equiv \begin{cases} 0 & \text{if } n + m = \text{even integer} \\ 1 & \text{if } n + m = \text{odd integer.} \end{cases}$$

The symmetry of the relations (18) reveals that they can both be satisfied only if

$$b_n = a_n(-1)^{n+1}. \tag{19}$$

Then the relations are identical; either constitutes a closed set of N linear equations for the N Fourier coefficients. Such a system will have a solution for non-zero Fourier coefficients provided that the determinant of the coefficients vanishes. Substituting (19) into (18), the matrix of coefficients is found to be

$$\mathbb{A}_{nm} \equiv \chi_i(-1)^m \frac{4\pi nm}{m^2 - n^2} \epsilon_{nm} + \left(\frac{1}{2} L\pi^2 n^2 + \frac{2\pi^2}{L} \chi_i + \frac{1}{2} L\pi^6 n^6 \mathrm{T}\right)\delta_{nm}, \tag{20}$$

and we require that

$$\mathrm{Det}|\mathbf{A}| = 0.$$

It may be seen that the parameter T only appears in the diagonal elements of the matrix $\mathbf{A}$, and if each row of $\mathbf{A}$ is divided through by $\frac{1}{2}L\pi^6 n^6$, then $-\mathrm{T}$ will be an eigenvalue of $\mathbf{A}$. Since $\mathbf{A}$ is symmetric, all eigenvalues will be real and that eigenvalue corresponding to the largest positive value of T is taken to be the root of physical interest.

The same procedure may be used to find the characteristic values and eigenfunctions of (10) for case (ii). When the Fourier series (16) is truncated to N terms and used to represent ψ in (15), and T is maximized with respect to each of the Fourier coefficients a_n and b_n, we obtain two sets of N linear equations:

$$4\pi\chi_{ii} \sum_{m=1}^{N} \left(\frac{nm}{m^2 - n^2}\right)\epsilon_{nm} b_m - \tfrac{1}{2}L[n^2\pi^2 + \mathrm{T}(n^2\pi^2 + l^2)^3]a_n = 0,$$

$$-4\pi\chi_{ii} \sum_{m=1}^{N} \left(\frac{nm}{m^2 - n^2}\right)\epsilon_{nm} a_m - \tfrac{1}{2}L[n^2\pi^2 + \mathrm{T}(n^2\pi^2 + l^2)^3]b_n = 0.$$

It is once again evident that $b_n = a_n(-1)^{n+1}$. If the Fourier coefficients are nonzero, then the determinant of the matrix of coefficients must vanish. The coefficient matrix in this case is

$$\mathbb{A}_{nm} \equiv \chi_{ii}(-1)^{m+1} \frac{4\pi nm}{n^2 - m^2} \epsilon_{nm} + \tfrac{1}{2}L\left[n^2\pi^2 + \mathrm{T}\left(n^2\pi^2 + \frac{4\pi^2}{L^2}\right)^3\right]\delta_{nm}. \tag{21}$$

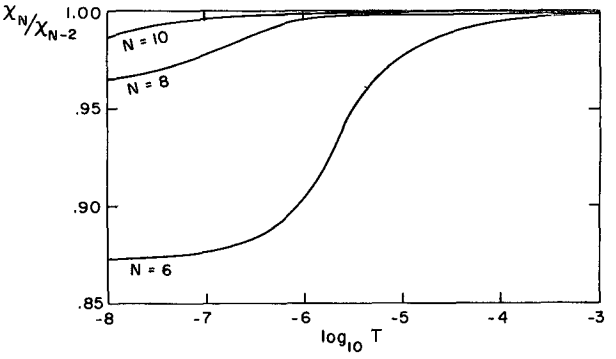

FIG. 1. Ratio of the Nth order variational approximation of the critical shear χ_i to the approximation of two orders lower for various values of N. Boundaries are free-slip.

The eigenvalues and eigenvectors of (20) are found using a standard matrix solver; the two-term approximation of (20) is also solved by hand as a check on the numerics. A sufficient number of terms is taken to determine the eigenvalue T to at least three significant figures. The entire process is repeated for various values of the horizontal wavelength L to find that mode which first becomes unstable as the fluid is destabilized.

The number of terms in (20) needed to determine the critical value of T (maximized with respect to L) to three significant figures is found to depend on the value of T itself, with only three or four terms needed when $\mathrm{T} \geq 10^{-4}$ increasing to ~ 10 when $\mathrm{T} = 10^{-8}$. As T approaches zero, the structure of the most unstable mode tends toward the inviscid result for which the most unstable wavenumber is infinity. The rapidly oscillatory nature of the nearly inviscid solutions therefore requires that many terms of the Fourier series (16) be included in order that ψ is accurately represented.

As an illustration of the convergence of the eigenvalues of (20) as the dimension of the matrix [i.e., the number of terms in (16)] is increased, we first adjust (20) so that χ_i is the matrix eigenvalue, and compare the Nth order approximation of χ_i with the approximation of two orders lower; this ratio being a function of T. Fig. 1 shows that the rapidity of the convergence of the eigenvalue χ_i for increasing N increases monotonically with T. We may suppose, on the basis of Fig. 1, that only two or three terms of the series (16) need be used to describe the asymptotic behavior of the streamfunction and associated eigenvalue χ_i as $\mathrm{T} \to \infty$. When (20) is truncated to a two by two matrix, the eigenvalues are easily computed by hand and one finds that

$$\chi_i \to 10950\,\mathrm{T} \quad \text{as} \quad \mathrm{T} \to \infty, \quad \text{when} \quad L = 7.5. \tag{22}$$

Here L has been chosen to minimize the coefficient of T in (22).

For case (ii) (neutral stratification), one may proceed in a similar fashion by solving the matrix (21) for the eigenvalues and eigenvectors, taking the matrix dimension N to be sufficiently large to insure reasonable precision of the eigenvalue. As this problem has been solved exactly by Kuo (1954), however, we solve for the eigenvalues of (21) to third order only and compare this solution with the exact results of Kuo (1954). The third-order determinant of (21) is easily obtained by hand, with the result

$$\chi_{ii}^2 = \left(\frac{5\pi L}{48}\right)^2 \left\{ \frac{\left[1 + \mathrm{T}'\left(1 + \frac{4}{L^2}\right)^3\right]\left[4 + \mathrm{T}'\left(4 + \frac{4}{L^2}\right)^3\right]\left[9 + \mathrm{T}'\left(9 + \frac{4}{L^2}\right)^3\right]}{\left[1 + \mathrm{T}'\left(1 + \frac{4}{L^2}\right)^3\right] + \left(\frac{5}{9}\right)^2\left[9 + \mathrm{T}'\left(9 + \frac{4}{L^2}\right)^3\right]} \right\}, \tag{23}$$

where $\mathrm{T}' \equiv \pi^4 \mathrm{T}$.

The asymptotic solution of (23) for large T is

$$\chi_{ii} \to 2747\mathrm{T} \quad \text{as} \quad \mathrm{T} \to \infty, \quad \text{when} \quad L = 3.41, \tag{24}$$

where again, that L has been chosen which minimizes the coefficient of T in (24).

Table 2 compares the critical value of χ_{ii} derived from (23) and minimized with respect to L with the results of Kuo (1954). Kuo's formulation of the problem is identical to that presented here, although horizontal shear is not considered. The errors in the third-order approximation of χ_{ii} range from ~7.5% when $\mathrm{T} = 10^{-6}$ to less than 0.1% when $\mathrm{T} = 10^{-2}$; the largest errors again occur for small T as the spatial variation of the streamfunction becomes large and exceeds the capacity of the truncated series (16) to adequately describe its structure.

The eigenvalues and eigenfunctions of (9) and (10) associated with free-slip boundaries and obtained using the variational method will be presented in Section 5.

b. No-slip boundaries

In deriving a variational method applicable to no-slip boundaries, it proves convenient to express the boundary conditions as constraints on ψ alone.

For case (i), the steady forms of (1)–(5) may be cross-differentiated to yield expressions for the second derivatives in y of u and $\partial p/\partial z$. In dimensionless form, these are

$$\frac{\partial^2 u}{\partial y^2} = (\chi_i - 2 - \sigma)\frac{\partial \psi}{\partial y} - \mathrm{T}\frac{\partial^5 \psi}{\partial y \partial z^4} + \left(1 - \frac{1+\sigma}{\chi_i}\right)\left(\frac{\partial \psi}{\partial z} + \mathrm{T}\frac{\partial^5 \psi}{\partial z^5}\right), \tag{25}$$

$$\frac{\partial^2}{\partial y^2}\frac{\partial p}{\partial z} = (\chi_i - 1 - \sigma)\frac{\partial \psi}{\partial y} - \mathrm{T}(1+\sigma)\frac{\partial^5 \psi}{\partial y \partial z^4} + \frac{\partial \psi}{\partial z} + \mathrm{T}\frac{\partial^5 \psi}{\partial z^5}. \tag{26}$$

Here u and $\partial p/\partial z$ have been nondimensionalized as follows:

$$\left.\begin{aligned} u^* &= u\frac{\nu}{H\tilde{\eta}}(1+\sigma) \\ \left(\frac{\partial p}{\partial z}\right)^* &= \left(\frac{\partial p}{\partial z}\right)\frac{\nu}{f\bar{U}_z H^2}\chi_i \end{aligned}\right\}, \tag{27}$$

where the asterisks denote the dimensional variables. Two constants of integration involved in the derivation of (25) and (26) have been set equal to zero to exclude the geostrophic solution

$$\psi = 0,$$
$$u = -\partial p/\partial y.$$

The requirement that u and $\partial p/\partial z$ vanish at the boundaries together with ψ and $\partial \psi/\partial z$ is equivalent, by (25) and (26), to requiring that

$$\psi = \frac{\partial \psi}{\partial z} = \frac{\partial^4 \psi}{\partial z^4} = \frac{\partial^5 \psi}{\partial z^5} = 0 \quad \text{at} \quad z = 0, 1. \tag{28}$$

The uneven nature of these conditions necessitates the construction of a new variational method. Rather than proceed with the derivation of such a method, we will simply state that the function ψ which maximizes T as expressed by

$$\mathrm{T} = \frac{-\frac{1}{\chi_i}\int_0^1\int_0^L\left(\frac{\partial \psi}{\partial z} + \frac{1}{2}\chi_i\frac{\partial \psi}{\partial y} + \mathrm{T}\frac{\partial^5 \psi}{\partial z^5}\right)^2 + \left(\frac{\chi_i}{4} - 1\right)\int_0^1\int_0^L\left(\frac{\partial \psi}{\partial y}\right)^2}{\int_0^1\int_0^L\left(\frac{\partial^3 \psi}{\partial y \partial z^2}\right)^2} \equiv \frac{I_1}{I_2} \tag{29}$$

is a solution of the characteristic value equation (9), together with the conditions (28). The proof of this theorem is provided in Appendix B.

In order to utilize the variational relation (29), we again represent ψ by a complete series of orthogonal functions which satisfies, term by term, the boundary conditions (28) and is periodic in y. It proves convenient, in constructing such a series, to shift the coordinate system so that the boundaries lie at $z = \pm\frac{1}{2}$. We then choose, as the orthogonal functions, the eigenfunctions of the equation

$$\frac{d^4G}{dz^4} = \alpha_i^4 G \tag{30}$$

subject to the conditions

$$G = \frac{dG}{dz} = \frac{d^4G}{dz^4} = \frac{d^5G}{dz^5} = 0 \quad \text{at} \quad z = -\tfrac{1}{2}, \tfrac{1}{2}, \tag{31}$$

where the α_i's are eigenvalues of (30).

There are an infinite number of eigenfunctions satisfying (30) and (31) corresponding to an infinite set of eigenvalues α; these eigenfunctions may be divided into the odd and even sets

$$\left.\begin{aligned} S_m &\equiv \frac{\sin\mu_m z}{\sin\mu_m/2} - \frac{\sinh\mu_m z}{\sinh\mu_m/2} \\ C_m &\equiv \frac{\cos\lambda_m z}{\cos\lambda_m/2} - \frac{\cosh\lambda_m z}{\cosh\lambda_m/2} \end{aligned}\right\}, \tag{32}$$

where the μ_m's and λ_m's are roots of

$$\left.\begin{aligned} \coth\frac{\mu}{2} - \cot\frac{\mu}{2} &= 0 \\ \tanh\frac{\lambda}{2} + \tan\frac{\lambda}{2} &= 0 \end{aligned}\right\}.$$

It is readily shown that the functions (32) satisfy the orthogonality conditions

$$\int_{-1/2}^{1/2} S_m S_n dz = \int_{-1/2}^{1/2} C_m C_n dz = \delta_{nm},$$

$$\int_{-1/2}^{1/2} S_m C_n dz = 0.$$

It is now possible to construct a complete orthogonal series describing ψ which is arbitrary except that it meets the boundary conditions (28) and is periodic in y:

$$\psi = \sum_{m=1}^{\infty} (a_m S_m \sin ly + b_m C_m \cos ly), \tag{33}$$

where a_m and b_m are constant coefficients which will be treated as variational parameters.

The above is substituted into the integral relation (29) and T is maximized with respect to each of the coefficients a_m and b_m. This leads to the two sets of relations

$$\left.\begin{aligned} \frac{\partial I_1}{\partial a_m} - \mathrm{T}\frac{\partial I_2}{\partial a_m} &= 0 \\ \frac{\partial I_1}{\partial b_m} - \mathrm{T}\frac{\partial I_2}{\partial b_m} &= 0. \end{aligned}\right\}, \quad m = 1, 2, 3 \ldots \infty. \tag{34}$$

When the series (33) is truncated to M terms, the extremization of T with respect to each a_m and b_m results in two sets of M linear equations for the coefficients. Performing the integrals and the operations (34), these sets are

$$a_n(1 + \mathrm{T}\mu_n^4)l^2\chi_i + \sum_{m=1}^{M} \{a_m[\overline{S_n'S_m'}](1 + \mathrm{T}\mu_n^4) \times (1 + \mathrm{T}\mu_m^4) + b_m l\chi_i[\overline{S_nC_m'}] \times [1 + \tfrac{1}{2}\mathrm{T}(\mu_n^4 + \lambda_m^4)]\} = 0, \tag{35a}$$

$$b_n(1 + \mathrm{T}\lambda_n^4)l^2\chi_i + \sum_{m=1}^{M} \{b_m[\overline{C_n'C_m'}] \times (1 + \mathrm{T}\lambda_n^4)(1 + \mathrm{T}\lambda_m^4) + a_m[\overline{S_mC_n'}]l\chi_i \times [1 + \tfrac{1}{2}\mathrm{T}(\lambda_n^4 + \mu_m^4)]\} = 0, \tag{35b}$$

$$n = 1, 2, 3 \ldots M.$$

The bracketed quantities are integrals of the products of various derivatives of S_m and C_m and are defined in Table 3.

With T specified, χ_i may be regarded as an eigenvalue of the matrix of coefficients of a_n and b_n associated with (35) after performing the following operations: we first define a new horizontal wavenumber as $l' \equiv l\chi_i$. Each row of the M equations in sets (35a) and (35b) are then divided through by $l'^2(1 + \mathrm{T}\mu_n^4)$ and $l'^2(1 + \mathrm{T}\lambda_n^4)$ respectively, resulting in the two sets

$$\frac{a_n}{\chi_i} + \sum_{m=1}^{M} \left\{\frac{a_m}{l'^2}[\overline{S_n'S_m'}](1 + \mathrm{T}\mu_m^4) + \frac{b_m}{l'}[\overline{S_nC_m'}]\left[\frac{1 + \tfrac{1}{2}\mathrm{T}(\mu_n^4 + \lambda_m^4)}{1 + \mathrm{T}\mu_n^4}\right]\right\} = 0, \tag{36a}$$

TABLE 2. Comparison of Kuo's (1954) solutions for the critical shear and horizontal wavelength characterizing the onset of instability in a neutrally stratified flow with those obtained using a variational method to third order.

T	χ_{ii} (Kuo)	χ_{ii} (Variational)	L (Kuo)	L (Variational)
10^{-6}	0.603	0.648	0.51	0.52
10^{-5}	1.007	1.065	0.80	0.79
10^{-4}	2.026	2.098	1.29	1.29
10^{-3}	6.100	6.146	2.07	2.07
10^{-2}	32.880	32.907	2.94	2.95

TABLE 3. Definitions of the bracketed quantities which appear in (35).

$$[\overline{S_n'S_m'}] \equiv \int_{-1/2}^{1/2} \frac{\partial S_n}{\partial z}\frac{\partial S_m}{\partial z} = \begin{cases} \dfrac{8\mu_n^2\mu_m^2\left[\mu_n \cot\dfrac{\mu_n}{2} - \mu_m \cot\dfrac{\mu_m}{2}\right]}{\mu_m^4 - \mu_n^4}, & n \neq m \\ \mu_m \cot\dfrac{\mu_m}{2}\left[\mu_m \cot\dfrac{\mu_m}{2} - 2\right], & n = m \end{cases}$$

$$[\overline{C_n'C_m'}] \equiv \int_{-1/2}^{1/2} \frac{\partial C_n}{\partial z}\frac{\partial C_m}{\partial z} = \begin{cases} \dfrac{8\lambda_n^2\lambda_m^2\left[\lambda_m \tan\dfrac{\lambda_m}{2} - \lambda_n \tan\dfrac{\lambda_n}{2}\right]}{\lambda_m^4 - \lambda_n^4}, & n \neq m \\ \lambda_n \tan\dfrac{\lambda_n}{2}\left[\lambda_n \tan\dfrac{\lambda_n}{2} + 2\right], & n = m. \end{cases}$$

$$[\overline{S_nC_m'}] \equiv \int_{-1/2}^{1/2} S_n \frac{\partial C_m}{\partial z} = \frac{-8\mu_n^2\lambda_m^2}{\mu_n^4 - \lambda_m^4}$$

$$\frac{b_n}{\chi_i} + \sum_{m=1}^{M}\left\{\frac{b_m}{l'^2}[\overline{C_n'C_m'}](1 + T\lambda_m^4) + \frac{a_m}{l'}[\overline{S_mC_n'}]\left[\frac{1 + \tfrac{1}{2}T(\lambda_n^4 + \mu_m^4)}{1 + T\lambda_n^4}\right]\right\} = 0, \quad (36b)$$

$$n = 1, 2, 3 \ldots M.$$

The above are now arranged in such a way that the quantity $-1/\chi_i$ is an eigenvalue of the associated matrix of coefficients. This matrix will have dimensions $2M \times 2M$ with the first M rows comprised of the coefficients in (36a), while the second M rows contain the coefficients of (36b). The coefficients of the a_n's are placed in the left half and those of the b_n's in the right half of the matrix. The matrix of coefficients, A_{ij} for which $-1/\chi_i$ is an eigenvalue is then defined as follows:

(i) For $i \leq M$

(a) For $j \leq M$

$$A_{ij} \equiv \frac{[\overline{S_i'S_j'}]}{l'^2}[1 + T\mu_j^4]$$

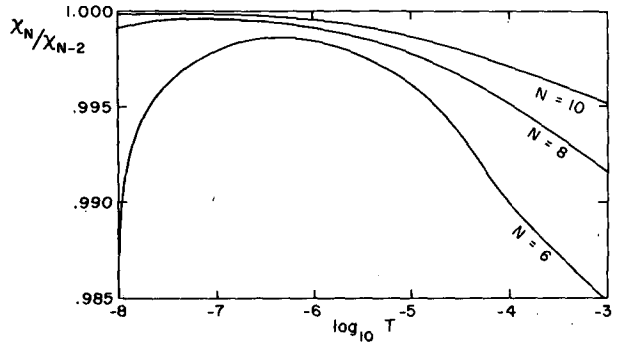

FIG. 2. As in Fig. 1 except for no-slip boundaries. Note the different scaling of the ordinate.

(b) For $j > M$

$$A_{ij} \equiv \frac{[\overline{S_iC_{j-M}'}]}{l'}\frac{1 + \tfrac{1}{2}T(\mu_i^4 + \lambda_{j-M}^4)}{1 + T\mu_i^4}$$

(ii) For $i > M$

(a) For $j \leq M$

$$A_{ij} \equiv \frac{[\overline{S_jC_{i-M}'}]}{l'}\frac{1 + \tfrac{1}{2}T(\lambda_{i-M}^4 + \mu_j^4)}{1 + T\lambda_{i-M}^4}$$

(b) For $j > M$

$$A_{ij} \equiv \frac{[\overline{C_{i-M}'C_{j-M}'}]}{l'^2}[1 + T\lambda_{j-M}^4].$$

The largest positive eigenvalue $1/\chi_i$ is found from the matrix thus defined using the numerical methods described previously. The value of $1/\chi_i$ is also maximized with respect to the wavenumber l'. In this instance, a manual calculation is only practical when $M = 1$ but, nevertheless, provides a valuable check of the numerical scheme and computer program.

It is again found that the number of terms necessary to determine χ_i to three significant figures is a function of T, but unlike the results for free-slip boundaries, the rapidity of the convergence is not a monotonic function of T. Fig. 2 illustrates that the ratio of the Nth order approximation of χ_i to that of two orders lower reaches a maximum at a finite value of T and that the convergence is generally faster for the no-slip case, at least when $T < 10^{-5}$. (Note the different scales of the ordinates in Figs. 1 and 2.) This behavior is related to both the structural complexity of the streamfunctions (with complex functions requiring many terms in the series representation) and the rate of convergence of the series for various derivatives of the streamfunction. In reference to the latter, it is apparent that

the rate of convergence of either of the series will be smaller for higher derivatives of the streamfunctions. Note that the variational relation (29) applicable to no-slip boundaries involves five derivatives in z, while the relation (14) for free-slip boundaries requires only three derivatives. Qualitatively, one would expect the convergence to be faster in the free-slip case for this reason, and indeed this is the case for large T (T multiples the highest derivatives). To understand why the reverse is true for small T, we first note that the most unstable inviscid mode represented by (11) is such that the order of magnitude of various derivatives of ψ at the boundary satisfies

$$\frac{\partial^r \psi}{\partial z^r} \sim O(l^{r-1}) \quad \text{as} \quad l \to \infty, \quad \text{at} \quad z = 0, 1. \tag{37}$$

One would expect the viscous solutions to satisfy this relation in the limit of vanishing T. The no-slip conditions demand that ψ and its *first* and fourth derivatives vanish at the boundaries, while the free-slip conditions require that ψ and its *second* and fourth derivatives vanish. By (37), one can see that the no-slip viscous solution approaches the inviscid result more rapidly than does the free-slip solution as $T \to 0$, hence the variational solution converges more rapidly in the former case for small T.

As another illustration of the rapidity of the convergence of the variational solution for no-slip boundaries, Table 4 lists the first five coefficients a_n and b_n for $T = 10^{-4}$.

c. The zonal velocity and temperature perturbations

Having obtained orthogonal series representations of the streamfunction in case (i) for free-slip and no-slip boundaries, it is now possible to construct solutions for the zonal velocity and temperature perturbations, the latter of which is proportional to $\partial p/\partial z$ in the hydrostatic case. The determination of u and p directly from (1) and (4) is not possible, however, as the uniform convergence of either of the truncated series (16) or (33) is not guaranteed for all of its derivatives and integrals. It is therefore necessary to construct elliptic equations relating the variables u and p to the streamfunction ψ which must appear in such a form that its various derivatives and integrals are adequately represented by the truncated orthogonal series. The series involved in these equations will converge most rapidly when its integrals and derivatives satisfy *term by term* the boundary conditions on u and p. For the no-slip case, (25) and (26) meet these requirements, while for free-slip boundaries, u and $\partial p/\partial z$ may be determined from

$$(1 + 1/\sigma)\frac{\partial^3 u}{\partial z^3} = \frac{\partial^2 \psi}{\partial z^2} - \frac{\chi_i}{\sigma}\frac{\partial^2 \psi}{\partial y^2} - \frac{T}{\sigma}\frac{\partial^6 \psi}{\partial z^6}, \tag{38}$$

TABLE 4. First five coefficients of the orthogonal series (33) for no-slip boundaries and $T = 10^{-4}$. Coefficients are normalized by a_1.

n	a_n	b_n
1	1.0000	1.0912
2	0.0105	−0.2785
3	0.0029	−0.0123
4	0.0006	−0.0016
5	0.0002	−0.0003

$$\frac{\partial^4 p}{\partial y \partial z^3} = \chi_i \frac{\partial^2 \psi}{\partial y^2} - \sigma \frac{\partial^2 \psi}{\partial z^2} - \sigma T \frac{\partial^6 \psi}{\partial z^6}, \tag{39}$$

where u and p have been normalized as in (27). Note that the Prandtl number appears explicitly in the above relations. In the results presented in the following section, the Prandtl number is set equal to unity in the calculation of u and p.

5. Results of the stability analysis

The methods described in the preceding section have been used to derive the characteristic values and eigenfunctions of (9) and (10) for free-slip and no-slip boundaries, with the characteristic values χ determined to at least three significant figures in the range $T \geq 10^{-8}$, except that for case (ii) a lower order approximation is intentionally used and the solutions compared with the exact results of Kuo (1954). The solutions of (9) and (10) yield the critical values of the shear parameter χ and the associated streamfunctions characterizing the onset of non-oscillatory instability, with the horizontal wavenumber chosen so as to minimize χ.

Fig. 3 shows the critical value of χ_i as a function of the viscous parameter T for both free-slip and no-slip boundaries. As one would expect, the critical value of χ_i increases monotonically with increasing T and the relationship becomes linear for large T as suggested by the asymptotic analysis. The asymptotic solutions of Walton (1975), valid when $(\pi^4 T)^{1/3} \ll 1$, are also depicted; the agreement is quite good in the region where Walton's results are valid.

When the diffusion is small, the type of boundary condition has little influence on the criterion for instability, but it comes as some surprise that when T is large, the instability sets in at smaller values of the shear for no-slip boundaries than it does when the boundaries are free-slip. This paradox is likely explained by the greater rotational damping of the instability at free-slip boundaries, which permit large zonal velocities to build up near the boundaries. This damping mechanism is also apparent in Rayleigh convection with rotation; the critical Rayleigh number in this case is smaller for no-slip boundaries when the diffusion is small (see, e.g., Chandrasekhar, 1961, p. 96). The striking difference

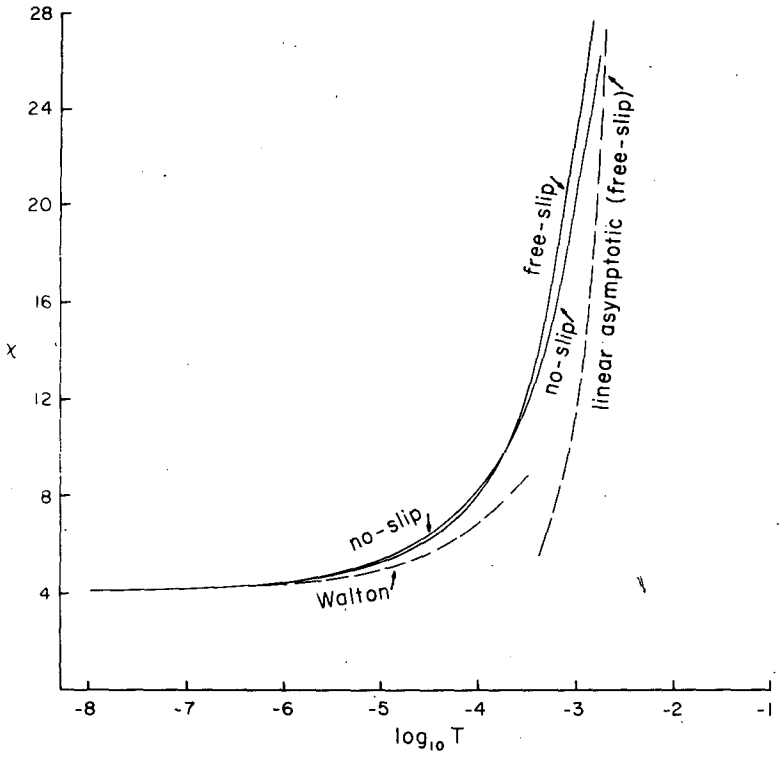

FIG. 3. Critical value of χ_i as a function of T for both sets of boundary conditions. Asymptotic results of Walton (1975) for small T, and asymptotic solution (for large T and free-slip boundary conditions) obtained using a variational method to second order are denoted by dashed lines.

between the zonal velocity structures associated with free-slip and no-slip boundaries (Fig. 8) supports this inference.

The relationship between the critical value of χ_{ii} and T for case (ii) (neutral stratification) and free-slip boundaries is illustrated in Fig. 4. The solution obtained using a variational method to third order is presented together with the exact solution by Kuo (1954). The comparison is quite good, especially for large T. These results are applicable for flow on an f plane which is perpendicular to the gravitational vector; in Appendix C we also consider the effect of the component of the rotation vector which lies in the meridional plane. So long as one may neglect the variation of the rotation vector with latitude ($\beta = 0$), the effects of the meridional component of rotation may be taken into account simply by redefining the critical shear parameter and the horizontal scaling; the perturbation equation remains the same. As is shown in Appendix C, the influence of the meridional component of rotation on the characteristics of the instability is very small, even when the flow is neutrally stratified.

The non-dimensional wavelength L characterizing the onset of instability in case (i) is shown as a function of T in Fig. 5. The value of L is order unity for T as small as 10^{-8}, illustrating the important result that *the proper scaling for the horizontal wavelength of inertial disturbances is not a viscous one except for extremely small diffusion. Rather, the wavelength of the disturbance is related to the depth of the unstable region and the slope of isentropic surfaces*. [The horizontal scale has been normalized by the ratio of the fluid depth and the slope of isentropic surfaces in order to arrive at Eq. (9).] As the viscosity is increased, the wavelengths approach asymptotic limits of 7.5 and 3.0 for free-slip and no-slip boundaries, respectively. The greater dissipation at no-slip boundaries apparently discourages large wavelengths.

The small dependence of the disturbance wavelength on the diffusion is particularly important so far as geophysical flows are concerned. In the atmosphere, the diffusion acting on mesoscale circulations is accomplished primarily by turbulence rather than molecular motions and, as such, the exact criteria obtained here are inapplicable. As the horizontal scale of the circulations is largely independent of the diffusion, however, the scale determined in this analysis should apply to geophysical circulations as well, so long as the turbulence acts to transport heat and momentum down gradient.

The horizontal wavelength characterizing the on-

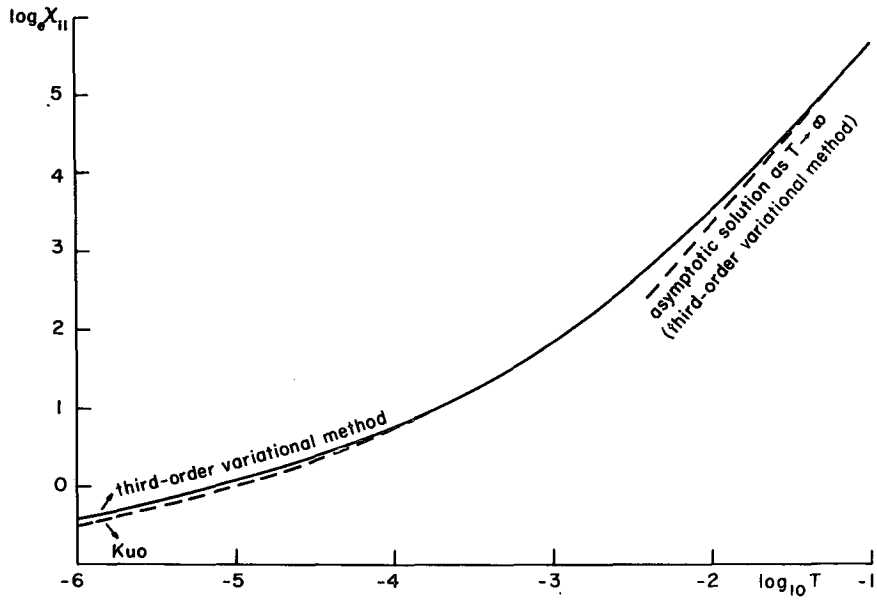

FIG. 4. Critical value of χ_{ii} as a function of T (for free-slip boundary conditions) derived using a variational method to third order. The exact solution by Kuo (1954) is indicated by dashed lines.

set of instability in case (ii) is illustrated, as a function of T, in Fig. 6; in this case the results are indistinguishable from the exact solution by Kuo (1954), at least when $T > 10^{-6}$. It is again evident that the disturbance rapidly acquires a horizontal scale on the order of the depth of the fluid as the viscosity is increased from zero, with L reaching an asymptotic limit of ~3.41.

Streamfunctions associated with the onset of instability in case (i) are presented in Fig. 7 for free-slip and no-slip boundaries, each for two values of T. The horizontal wavelength in each instance is that

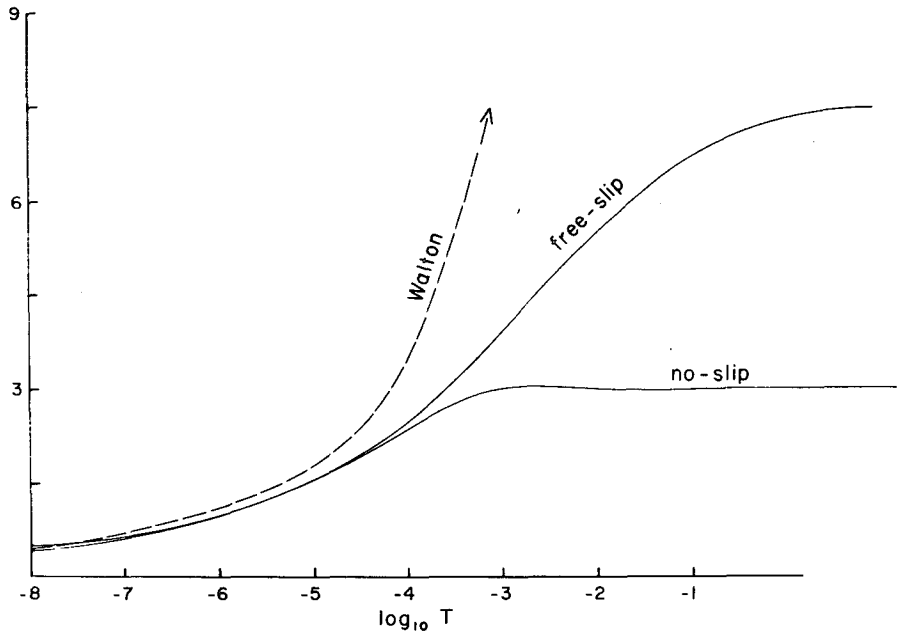

FIG. 5. Nondimensional wavelength L at which instability sets in, as a function of T for case (i) and both sets of boundary conditions. Asymptotic solutions for small T by Walton (1975) indicated by dashed line.

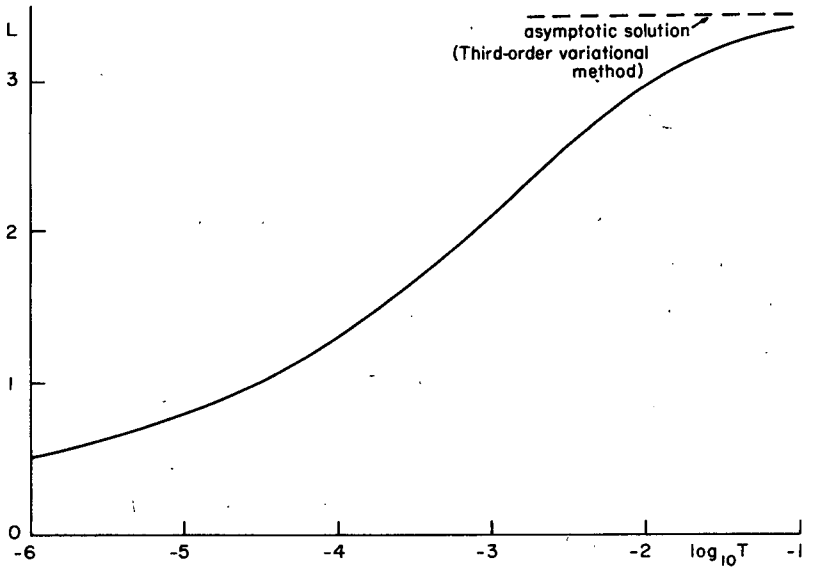

FIG. 6. Nondimensional wavelength L at which instability sets in, as a function of T for case (ii). The results of Kuo (1954) are identical.

which minimizes the critical value of χ_i for a given value of T. The sloped dashed line indicates the orientation of the potential isotherms when $\sigma = 1$, and the Ekman depth δ defined by

$$\delta \equiv \left(\frac{2\nu}{f}\right)^{1/2} = 2^{1/2} H \mathrm{T}^{1/4}$$

is depicted in the lower left portion of the diagrams.

The streamlines take the form of closed vortices elongated along isentropic surfaces, and substantial temperature advection is indicated near the boundaries. The slope of the trajectories is very nearly that of the isentropic surfaces when the boundaries are free-slip, but appears to be greater than the isentrope slope for no-slip boundaries, especially when T is large. The withdrawal of the circulation outside the boundary layer in the no-slip case is strongly apparent.

Of special interest are the fields of perturbation zonal velocity (Fig. 8) associated with the streamfunctions depicted in Fig. 7. These have been computed from (38) in the free-slip case, and (25) when the boundaries are no-slip; in all cases the Prandtl number is unity.

The contrasting structures of the zonal velocity components for the two sets of boundary conditions are striking. In the free-slip case, the maximum velocities are found at the boundaries near the point of intersection of the zero streamline, whereas the greatest zonal component occurs in the interior of the domain when the boundaries are no-slip. It is this buildup of large vorticities near the free-slip boundaries which we believe inhibits vertical motion through inertial damping and leads to higher critical shears for free-slip than for no-slip boundaries.

The zonal velocity perturbation is apparently dominated by Coriolis turning of the meridional wind in the free-slip case, and by vertical advection of the base state zonal wind when no-slip boundaries are present. For both boundary conditions, negative correlations of u and w, and of u and v are evident. The actual transport of zonal momentum must be downshear, since the instability converts zonal to eddy kinetic energy, but the net meridional flux of zonal momentum is probably poleward despite the first-order negative correlation of u and v, since the positive correlation of the second-order meridional flow and the base state zonal wind is dominant in this case, as shown by Walton (1975). In fact, the fully nonlinear inviscid instabilities, as long as they remain symmetric, must transport zonal momentum poleward in order to conserve Ertel potential vorticity, which may be defined for a Boussinesq fluid as

$$q \equiv [(\nabla \times \mathbf{V}) + \hat{\mathbf{k}} f] \cdot \nabla \ln\theta.$$

For symmetric flow in geostrophic balance,

$$\frac{\partial \ln\theta}{\partial z} \equiv \frac{N^2}{g}, \quad \frac{\partial \ln\theta}{\partial y} = -f\frac{\bar{U}_z}{g}.$$

Thus

$$q = \eta \frac{N^2}{g} - f\frac{\bar{U}_z^2}{g}.$$

If the instability acts to destroy the vertical shear, then if q is conserved the product ηN^2 must also decrease. The vertical heat fluxes correct to second order are upward, as shown by Stone (1972), and hence must act to increase N^2. Thus it must be true that the inviscid instability leads to a decrease in the absolute vorticity about the vertical axis; in the

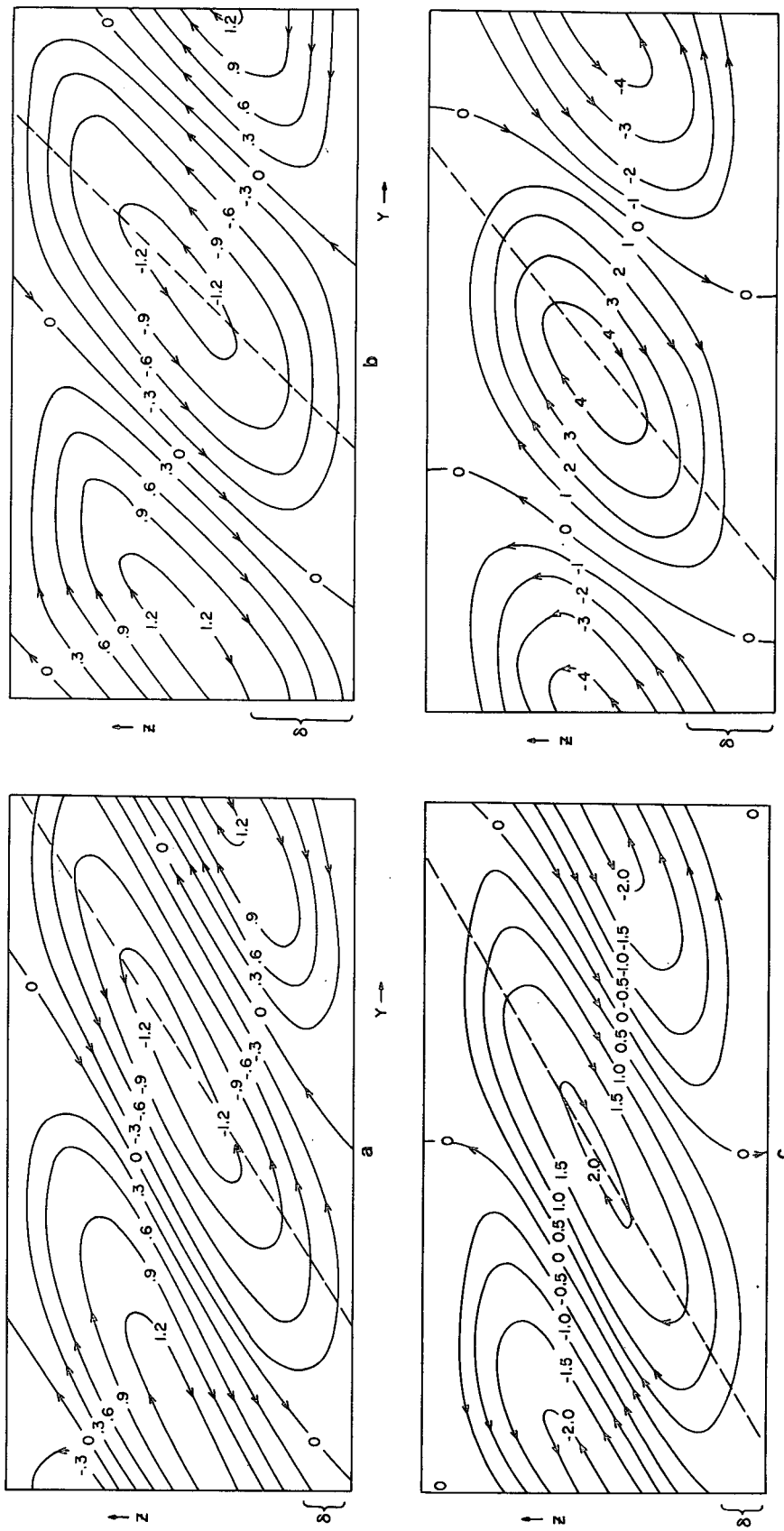

FIG. 7. Streamfunctions associated with the onset of instability. Solutions for free-slip boundaries are represented in (a) and (b) for $T = 10^{-4}$ and 1.6×10^{-3}, respectively, while (c) and (d) are for no-slip boundaries and $T = 10^{-4}$ and 10^{-3}, respectively. The abscissa spans one full wavelength, and the Ekman depth is indicated at lower left. Relative orientation of the potential isotherms where $\sigma = 1$ is illustrated by dashed line.

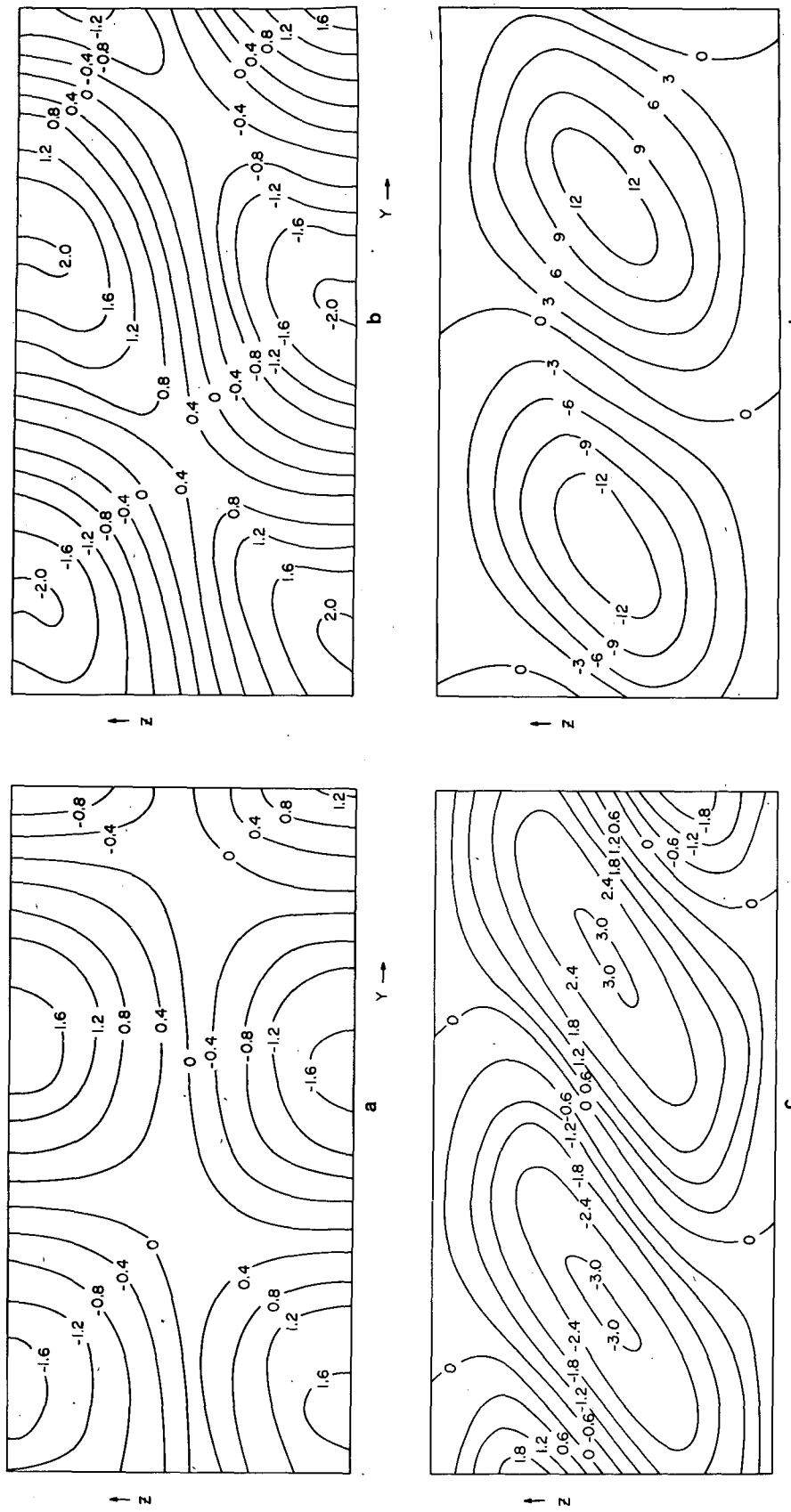

FIG. 8. Normalized perturbation zonal velocity fields associated with the streamfunctions in Fig. 7. Positive values denote flow out of the page, and $\sigma = 1$.

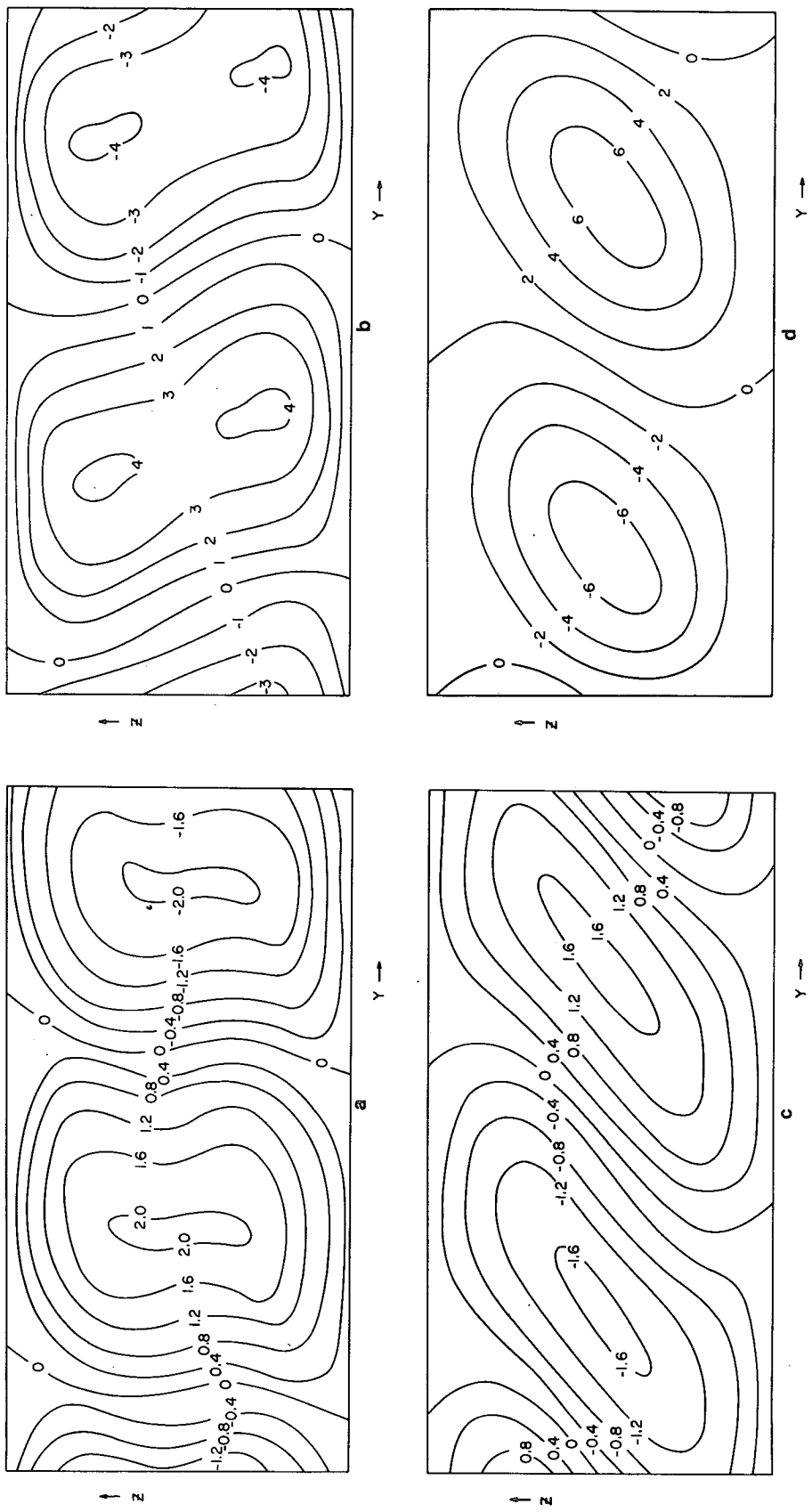

FIG. 9. Normalized temperature perturbation ($\partial p/\partial z$) associated with the streamfunctions in Fig. 7, with $\sigma = 1$.

symmetric case this implies a net poleward flux of zonal momentum. We may conclude that Walton's (1975) result that zonal momentum is always convected poleward for small-amplitude nearly inviscid symmetric instability is valid for the fully nonlinear motions as well. This result is called into question for the fully viscous solutions, however, since potential vorticity is not conserved and, more especially, as it appears that the eddy vertical heat flux may well be negative for certain values of T and σ. This is evident in the solutions for the perturbation potential temperature (proportional to $\partial p/\partial z$) derived from (39) in the free-slip case and (26) when the boundaries are no-slip. These fields are illustrated in Fig. 9, with the Prandtl number held at unity. For the range of T shown, a comparison of the temperature perturbations and streamfunctions reveals a downward eddy heat flux averaged over the domain, with high temperatures in the regions of descent and low temperatures where the motion is upward. Stone (1972) and Walton (1975) have shown that the total vertical transports of zonal momentum and heat, correct to second-order in an amplitude expansion, are identical to the eddy fluxes alone when the domain is meridionally unbounded, since the second-order circulation which develops has no vertical component and thus does not contribute to vertical advection. Hence, for at least some values of T and σ, inertial instability may lead to downward heat fluxes and lower static stability.

The pressure distribution near the boundaries may be inferred from Fig. 9 together with the symmetry of the circulations. High pressure occurs under the region of upward motion, with low pressure at the surface where the air is subsiding. For the values of T shown here, the perturbation pressure and zonal wind fields are nearly in geostrophic balance.

Finally, it is evident that most of the eddy kinetic energy is associated with the zonal component of the perturbation flow, at least when T is not large. In the results presented here, the maximum value of the ratio u/v (computed using the dimensional values of u and v) for free-slip boundaries and Prandtl number unity is 15 when $T = 10^{-4}$ and 4.8 when $T = 1.6 \times 10^{-3}$. When the boundaries are no-slip, this ratio is even larger, except near the top of the boundary layer.

6. Conclusions

Solution of the fully viscous, adiabatic and Boussinesq linear equations governing two-dimensional perturbations with axes along the vertical shear vector reveals an inertial instability which occurs when the Richardson number falls below a critical value which depends on the absolute vorticity of the flow and the diffusive properties of the fluid. The circulations described here set in as nonpropagating overturning motions; the possibility of oscillatory instability is not examined as earlier results of McIntyre (1969) and Walton (1975) indicate that such an instability is unlikely.

The principal finding of this analysis is that inertial circulations are inherently mesoscale in the sense that viscosity, rotation, horizontal gradients in the large-scale flow and ageostrophic advection all contribute to the dynamics of the motion. Viscosity acts in the singular sense that it assures that the most rapidly growing disturbance possesses a finite scale which itself is only a weak function of the dissipative properties of the fluid. This horizontal scale is the ratio of the depth of the unstable domain and the slope of isentropic surfaces. It seems safe to suppose that the result is applicable as well to geophysical flows in which the diffusive processes operate very differently from molecular diffusion.

The fully viscous inertial circulations are otherwise similar to the inviscid motions in that they transport zonal momentum downward and poleward; however, it appears that the vertical heat fluxes may be downward, depending on the diffusive properties of the fluid. Apparently, the most unstable mode chooses an orientation for which the motions do relatively little work against friction, at the expense of doing some work against gravity. It is possible, therefore, that inertial instability leads to local static destabilization.

The structure and scale of inertial circulations, together with the conditions under which they may occur, suggest a connection between inertial instability and certain mesoscale circulations in the atmosphere. Richardson numbers of order unity, however, are generally observed in small regions near the surface and close to jet streams, yet squall-line circulations extend through most of the troposphere. One would suspect that the addition of condensation alters the criteria for inertial instability as well as its structure. The effects of moisture on inertial circulations will be the subject of Part II.

Acknowledgments. I am sincerely grateful for the assistance afforded me by many of the faculty and staff of the Department of Meteorology at MIT, particularly Jule Charney who suggested the use of the variational approach in this problem, and Frederick Sanders, Peter Stone and David Andrews, whose advice was invaluable. Thanks are due Steven Ricci and Isabelle Kole of MIT, and Linda Howell and Joan Kimpel of Oklahoma University for their assistance in typing the manuscript and drafting the figures.

The author was supported by a grant from the National Science Foundation (76-20070 ATM) while conducting this research as part of his doctoral program at MIT.

APPENDIX A

Reduction of (6) to Sixth Order

The time-independent non-hydrostatic form of (6) may be written

$$-\kappa\nu^2(\nabla^2)^4\psi = \nu\nabla^2\left(f\bar{U}_z\frac{\partial^2\psi}{\partial y\partial z} + N^2\frac{\partial^2\psi}{\partial y^2}\right) + \kappa\nabla^2\left(f\bar{U}_z\frac{\partial^2\psi}{\partial y\partial z} + f\bar{\eta}\frac{\partial^2\psi}{\partial z^2}\right).$$

The above may be twice integrated to yield

$$-\kappa\nu^2(\nabla^2)^3\psi = (\nu+\kappa)f\bar{U}_z\frac{\partial^2\psi}{\partial y\partial z} + \nu N^2\frac{\partial^2\psi}{\partial y^2} + \kappa f\bar{\eta}\frac{\partial^2\psi}{\partial z^2} + \phi, \quad \text{(A1)}$$

where ϕ is a function whose Laplacian vanishes. By applying either set of boundary conditions, ϕ may be shown to vanish.

1. Free-slip boundaries

$$\psi = \frac{\partial^2\psi}{\partial z^2} = \frac{\partial u}{\partial z} = \frac{\partial p}{\partial z} = 0 \quad \text{at} \quad z = 0, H.$$

First, the perturbation density is eliminated between (3) and (4) to yield

$$\kappa\nabla^2\frac{1}{\rho_0}\frac{\partial p}{\partial z} = \kappa\nu(\nabla^2)^2\frac{\partial\psi}{\partial y} + f\bar{U}_z\frac{\partial\psi}{\partial z} + N^2\frac{\partial\psi}{\partial y}. \quad \text{(A2)}$$

(Hereafter, the perturbation pressure is normalized by ρ_0.)

The above is differentiated once in y, while (1) is differentiated once in z and (2) three times in z. The result is

$$\kappa\nabla^2\frac{\partial^2 p}{\partial y\partial z} = f\bar{U}_z\frac{\partial^2\psi}{\partial y\partial z} + N^2\frac{\partial^2\psi}{\partial y^2} + \kappa\nu(\nabla^2)^2\frac{\partial^2\psi}{\partial y^2}, \quad \text{(A3)}$$

$$-\nu\nabla^2\frac{\partial u}{\partial z} = -\bar{\eta}\frac{\partial^2\psi}{\partial z^2} - \bar{U}_z\frac{\partial^2\psi}{\partial y\partial z}, \quad \text{(A4)}$$

$$-\nu\nabla^2\frac{\partial^4\psi}{\partial z^4} = \frac{\partial^4 p}{\partial y\partial z^3} + f\frac{\partial^3 u}{\partial z^3}. \quad \text{(A5)}$$

By differentiating (2) once in z, it is evident that $\partial^4\psi/\partial z^4 = 0$ on the free-slip boundaries, and utilizing the other three boundary conditions, it is evident that on the boundaries, the above become

$$\left.\begin{aligned}\kappa\frac{\partial^4 p}{\partial y\partial z^3} &= f\bar{U}_z\frac{\partial^2\psi}{\partial y\partial z}\\ \nu\frac{\partial^3 u}{\partial z^3} &= \bar{U}_z\frac{\partial^2\psi}{\partial y\partial z}\\ -\nu\frac{\partial^6\psi}{\partial z^6} &= \frac{\partial^4 p}{\partial y\partial z^3} + f\frac{\partial^3 u}{\partial z^3}\end{aligned}\right\} \quad \text{at} \quad z = 0, H.$$

Combining the above, we obtain

$$-\nu^2\kappa\frac{\partial^6\psi}{\partial z^6} = f\bar{U}_z(\nu+\kappa)\frac{\partial^2\psi}{\partial y\partial z} \quad \text{at} \quad z = 0, H. \quad \text{(A6)}$$

By inspecting (A1), it is evident that ϕ must also vanish at the boundaries. As $\nabla^2\phi = 0$, the only function ϕ which satisfies these boundary conditions and is periodic in y is $\phi = 0$.

2. No-slip boundary conditions

$$\psi = \frac{\partial\psi}{\partial z} = u = \frac{\partial p}{\partial z} = 0 \quad \text{at} \quad z = 0, H.$$

If (1) is differentiated once in z, and the operator $\nu\nabla^2(\partial/\partial z)$ is applied to (2), we have together with (A3),

$$\nu\nabla^2\frac{\partial u}{\partial z} = \bar{\eta}\frac{\partial^2\psi}{\partial z^2} + \bar{U}_z\frac{\partial^2\psi}{\partial y\partial z},$$

$$f\nu\nabla^2\frac{\partial u}{\partial z} = -\nu\nabla^2\frac{\partial^2 p}{\partial y\partial z} - \nu^2(\nabla^2)^2\frac{\partial^2\psi}{\partial z^2},$$

$$\kappa\nabla^2\frac{\partial^2 p}{\partial y\partial z} = \kappa\nu(\nabla^2)^2\frac{\partial^2\psi}{\partial y^2} + f\bar{U}_z\frac{\partial^2\psi}{\partial y\partial z} + N^2\frac{\partial^2\psi}{\partial y^2}.$$

On the no-slip boundaries, the above become

$$\left.\begin{aligned}\nu\nabla^2\frac{\partial u}{\partial z} &= \bar{\eta}\frac{\partial^2\psi}{\partial z^2}\\ f\nu\nabla^2\frac{\partial u}{\partial z} &= -\nu\frac{\partial^4 p}{\partial y\partial z^3} - \nu^2(\nabla^2)^2\frac{\partial^2\psi}{\partial z^2}\\ \kappa\frac{\partial^4 p}{\partial y\partial z^3} &= \kappa\nu(\nabla^2)^2\frac{\partial^2\psi}{\partial y^2}\end{aligned}\right\} \text{at} \quad z = 0, H.$$

Eliminating u and p from the above, we arrive at

$$\nu^2(\nabla^2)^3\psi = -f\bar{\eta}\frac{\partial^2\psi}{\partial z^2} \quad \text{at} \quad z = 0, H.$$

Comparison with (A1) shows that again, $\phi = 0$ on the boundaries and as $\nabla^2\phi = 0$, ϕ must vanish everywhere.

APPENDIX B

Proof of the Variational Theorems

1. Free-slip boundaries

It may be shown that the maximization of T as expressed by (14), with respect to a function ψ which

satisfies free-slip boundary conditions, yields the solution of the perturbation equation (9).[4]

If T is to be maximized in (14), then a small variation in T with respect to ψ must satisfy

$$\delta T = \frac{1}{I_2}\left[\delta I_1 - \frac{I_1}{I_2}\,\delta I_2\right] = 0$$

or

$$\delta I_1 - T\delta I_2 = 0. \tag{B1}$$

From (14),

$$\delta I_1 = \int_0^1\int_0^L \left[\chi\left(\delta\psi\frac{\partial^2\psi}{\partial y\partial z} + \psi\delta\frac{\partial^2\psi}{\partial y\partial z} - 2\frac{\partial\psi}{\partial y}\,\delta\frac{\partial\psi}{\partial y}\right) - 2\frac{\partial\psi}{\partial z}\,\delta\frac{\partial\psi}{\partial z}\right].$$

Using integration by parts and applying the free-slip boundary conditions, the above becomes

$$\delta I_1 = \int_0^1\int_0^L \left[\chi\left(\frac{\partial^2\psi}{\partial y\partial z} + \frac{\partial^2\psi}{\partial y^2}\right) + \frac{\partial^2\psi}{\partial z^2}\right](2\delta\psi).$$

Similarly, the increment δI_2 may be expressed as

$$\delta I_2 = -\int_0^1\int_0^L \frac{\partial^6\psi}{\partial z^6}(2\delta\psi).$$

Finally, the relation (B1) becomes

$$\int_0^1\int_0^L \left[\chi\frac{\partial^2\psi}{\partial y\partial z} + \chi\frac{\partial^2\psi}{\partial y^2} + \frac{\partial^2\psi}{\partial z^2} + T\frac{\partial^6\psi}{\partial z^6}\right](2\delta\psi) = 0.$$

For an arbitrary variation $\delta\psi$ that satisfies the boundary conditions and which makes $\delta T = 0$, the above relation is satisfied only if the expression in brackets vanishes. This expression is the original characteristic value equation (9), which is therefore satisfied if T is maximized in (14).

[4] For the sake of brevity, the proof will be carried out only for the hydrostatic case (i); the proof of the variational theorem for case (ii) is similar.

2. No-slip boundaries

We here prove that when T, as expressed by (29), is maximized with respect to a function ψ which satisfies the boundary conditions

$$\psi = \frac{\partial\psi}{\partial z} = \frac{\partial^4\psi}{\partial z^4} = 0 \quad \text{at} \quad z = 0, 1,$$

that function which maximizes T is a solution of the characteristic value equation (9). It is shown in Section 4 that

$$\partial^5\psi/\partial z^5 = 0 \quad \text{at} \quad z = 0, 1$$

as well.

In order to simplify the proof, we here introduce a function F defined as

$$F \equiv -(\partial^2 p/\partial y\partial z).$$

From the boundary conditions, F must also vanish at the boundaries. If u and F are normalized by $\nu/H\bar{\eta}$ and $\nu/f\bar{\eta}$ respectively, the normalized time-independent forms of (1), (2) and (4) may be written for the hydrostatic case as

$$\frac{\partial^2 u}{\partial z^2} = \frac{\partial\psi}{\partial z} + \frac{1}{2}\chi\frac{\partial\psi}{\partial y}, \tag{B2}$$

$$F = \frac{\partial u}{\partial z} + T\frac{\partial^4\psi}{\partial z^4}, \tag{B3}$$

$$\frac{\partial^2 F}{\partial z^2} = -\frac{1}{2}\chi\frac{\partial^2\psi}{\partial y\partial z} - \chi\frac{\partial^2\psi}{\partial y^2}. \tag{B4}$$

Here (2) has been differentiated once in z to obtain (B3) and (4) has been differentiated in y to yield (B4). Taking one derivative of (B3) and eliminating u between (B3) and (B2), we find that

$$\frac{\partial F}{\partial z} = \frac{\partial\psi}{\partial z} + \frac{1}{2}\chi\frac{\partial\psi}{\partial y} + T\frac{\partial^5\psi}{\partial z^5}. \tag{B5}$$

Now the variational relation (29) may be rewritten in terms of F as

$$T = \frac{-\frac{1}{\chi}\int_0^1\int_0^L\left(\frac{\partial F}{\partial z}\right)^2 + \int_0^1\int_0^L\left(\frac{\chi}{4} - 1\right)\left(\frac{\partial\psi}{\partial y}\right)^2}{\int_0^1\int_0^L\left(\frac{\partial^3\psi}{\partial y\partial z^2}\right)^2} \equiv \frac{I_1}{I_2}. \tag{B6}$$

We now proceed to maximize T in (B6) with respect to ψ and $F(\psi)$:

$$\delta T = \frac{1}{I_2}[\delta I_1 - T\delta I_2] = 0. \tag{B7}$$

From (B6),

$$\delta I_1 = -\frac{2}{\chi}\int_0^1\int_0^L\frac{\partial F}{\partial z}\,\delta\frac{\partial F}{\partial z} + 2\left(\frac{\chi}{4} - 1\right)\int_0^1\int_0^L\frac{\partial\psi}{\partial y}\,\delta\frac{\partial\psi}{\partial y}.$$

An integration by parts together with boundary conditions on F and ψ yields

$$\delta I_1 = \frac{2}{\chi}\int_0^1\int_0^L F\delta\frac{\partial^2 F}{\partial z^2} + 2\left(\frac{\chi}{4} - 1\right)\int_0^1\int_0^L\frac{\partial\psi}{\partial y}\,\delta\frac{\partial\psi}{\partial y}.$$

Using (B4), this becomes

$$\delta I_1 = -\int_0^1\int_0^L F\left[\delta\frac{\partial^2\psi}{\partial y\partial z} + 2\delta\frac{\partial^2\psi}{\partial y^2}\right] + 2\left(\frac{\chi}{4}-1\right)\int_0^1\int_0^L \frac{\partial\psi}{\partial y}\,\delta\frac{\partial\psi}{\partial y}\,.$$

Applying integration by parts and boundary conditions to the terms on the right above yields

$$\delta I_1 = -\int_0^1\int_0^L\left[\frac{\partial^2 F}{\partial y\partial z} + 2\frac{\partial^2 F}{\partial y^2} + 2\left(\frac{\chi}{4}-1\right)\frac{\partial^2\psi}{\partial y^2}\right](\delta\psi).$$

Applying integration by parts to δI_2, we find that

$$\delta I_2 = \int_0^1\int_0^L 2\frac{\partial^3\psi}{\partial y\partial z^2}\,\delta\frac{\partial^3\psi}{\partial y\partial z^2} = -2\int_0^1\int_0^L\frac{\partial^6\psi}{\partial y^2\partial z^4}\,\delta\psi.$$

Using this pair of relations and one further integration by parts, the variational relation (B7) becomes

$$\int_0^1\int_0^L\left[\frac{\partial F}{\partial z} + 2\frac{\partial F}{\partial y} + 2\left(\frac{\chi}{4}-1\right)\frac{\partial\psi}{\partial y} - 2T\frac{\partial^5\psi}{\partial y\partial z^4}\right]\delta\frac{\partial\psi}{\partial y} = 0.$$

For an arbitrary variation $\delta(\partial\psi/\partial y)$ which fulfills the boundary conditions, the above may only be true if the expression in brackets vanishes.

Substituting (B5) for $\partial F/\partial z$ and (B3) for $\partial F/\partial y$ in the above, it is found that

$$\frac{\partial\psi}{\partial z} + \chi\frac{\partial\psi}{\partial y} + T\frac{\partial^5\psi}{\partial z^5} - 2\frac{\partial\psi}{\partial y} + 2\frac{\partial^2 u}{\partial y\partial z} = 0.$$

If the above is differentiated once in z and u is eliminated using (B2), then we arrive at

$$T\frac{\partial^6\psi}{\partial z^6} + \chi\frac{\partial^2\psi}{\partial y\partial z} + \chi\frac{\partial^2\psi}{\partial y^2} + \frac{\partial^2\psi}{\partial z^2} = 0,$$

which is the characteristic value equation (9). It is thus seen that a function ψ that satisfies the no-slip boundary conditions and maximizes T in the variational relation (29) is a solution of the characteristic value equation (9).

APPENDIX C

Inclusion of the Meridional Component of the Earth's Rotation

When the aspect ratio of inertial circulations is of order unity, one would expect that the meridional component of the Coriolis acceleration influences the instability. We here solve the eigenvalue problem for the condition of marginal stability with all components of the Coriolis acceleration included. Elementary scale analysis of the primitive equations shows that the terms involving the meridional component of the rotation vector are negligible except when the hydrostatic approximation breaks down. The perturbation equations are here derived with a finite static stability included as an illustration of this point.

We first consider the case in which the unperturbed flow is purely meridional. It is then easily shown that *provided that one may neglect the variation of f with latitude, the meridional component of the earth's rotation does not enter the perturbation equations for inertial instability.* This is so because we permit no variation along the axis of the inertial rolls, which in this case are aligned north–south. Thus the meridional component of the ambient rotation cannot influence the instability. The condition that the variation of f in latitude may be neglected is that the fractional change in f following the parcel motion is small during a time increment characterizing the growth of the instability. This may be written

$$\frac{\Delta f}{f} = \frac{df}{dt}\frac{\Delta t}{f} = V_0\beta\frac{\Delta t}{f} \ll 1,$$

where V_0 is a velocity scale, β is df/dy, and Δt is a characteristic time scale of the disturbance. Following McIntyre (1970), we take the latter to be $O[f^{-1/2}(V_0/H)^{-1/2}]$. Then the above condition becomes

$$\frac{H^{1/2}}{a}\left(\frac{V_0}{2\Omega}\right)^{1/2}\frac{\cos\varphi}{(\sin\varphi)^{3/2}} \ll 1,$$

where a is the mean radius of the earth and ϕ the latitude. Taking $H = 10$ km and $V_0 = 100$ m s^{-1}, we find that the left-hand side of the above is order unity at about 3° latitude and decreases to 0.2 at 10° latitude. Considering the liberal estimates of H and V_0, it seems safe to suppose that one may neglect the variation in f with latitude in this problem outside the tropics.

We next consider the case where the unperturbed flow is purely zonal. The Boussinesq equations for symmetric flow on an f plane may be written

$$\frac{du}{dt} = fv - f^*w + \nu\nabla^2 u, \tag{C1}$$

$$\frac{dv}{dt} = -\frac{1}{\rho_0}\frac{\partial p}{\partial y} - fu + \nu\nabla^2 v, \tag{C2}$$

$$\frac{dw}{dt} = -\frac{1}{\rho_0}\frac{\partial p}{\partial z} + B + f^*u + \nu\nabla^2 w, \quad \text{(C3)}$$

$$\frac{dB}{dt} = \kappa\nabla^2 B, \quad \text{(C4)}$$

$$\frac{\partial v}{\partial y} + \frac{\partial w}{\partial z} = 0, \quad \text{(C5)}$$

where $f^* \equiv 2\Omega\cos\phi$ and $B \equiv -g(\rho'/\rho_0)$ and the notation is otherwise the same.

We take as a base-state solution to this set

$$\left.\begin{aligned} \bar{v} &= \bar{w} = 0 \\ \bar{U}(y,z) &= \bar{U}_z z + \bar{U}_y y \\ \bar{B}(y,z) &= N_z^2 + \bar{B}_y y \end{aligned}\right\},$$

where $\bar{U}_z$, $\bar{U}_y$, N^2 and $\bar{B}_y$ are constants. We find from (C2) and (C3) that the thermal wind relation between $\bar{B}_y$ and $\bar{U}_z$ is

$$\bar{B}_y = -f\bar{U}_z - f^*\bar{U}_y. \quad \text{(C6)}$$

Proceeding as before, we find the time-independent form of the equations describing perturbations about this base state, analogous to (7), may be written

$$\begin{aligned} -\nu^2(\nabla^2)^3\psi &= f\bar{\eta}\frac{\partial^2\psi}{\partial z^2} + [\sigma N^2 + f^*(f^* + \bar{U}_z)] \\ &\times \frac{\partial^2\psi}{\partial y^2} + [f(2f^* + (1+\sigma)\bar{U}_z) \\ &+ f^*\bar{U}_y(\sigma - 1)]\frac{\partial^2\psi}{\partial y\partial z}. \end{aligned} \quad \text{(C7)}$$

In the special case that $f = \bar{U}_y = 0$, the above reduces to the Rayleigh convection problem with the single stability parameter

$$\mathrm{Ra}' = \mathrm{Ra} + \frac{f^*(f^* + \bar{U}_z)H^4}{\nu^2},$$

where Ra is the Rayleigh number. If $\bar{U}_z < -f^*$, the flow may become unstable at Rayleigh numbers below the usual critical value. When $\bar{U}_z < -f^*$ at the equator, the square of the angular momentum decreases radially outward and the flow is classically inertially unstable. If we require that

$$\sigma N^2 + f^*(f^* + \bar{U}_z) \geq 0$$

and scale z by H and y by

$$\left[\frac{\sigma N^2 + f^*(f^* + \bar{U}_z)}{f\bar{U}_z(1+\sigma) + 2ff^* + f^*\bar{U}_y(\sigma - 1)}\right]H,$$

the perturbation equation will reduce to the form (9) or (10) if we take the flow to be either hydrostatic or neutrally stratified. In the former case, we require that

$$\frac{f\bar{U}_z(1+\sigma) + 2ff^* + f^*\bar{U}_y(\sigma - 1)}{\sigma N^2 + f^*(f^* + \bar{U}_z)} \ll 1.$$

Then the stability parameter χ_i in (9) will be defined

$$\chi_i \equiv \frac{f}{\bar{\eta}} \times \frac{\left[(1+\sigma)\bar{U}_z + 2f^* + \frac{f^*}{f}\bar{U}_y(\sigma - 1)\right]^2}{\sigma N^2 + f^*(f^* + \bar{U}_z)}. \quad \text{(C8)}$$

Since in general $\bar{U}_z \gg f^*$ and $\bar{U}_z \gg \bar{U}_y$, the above is very nearly equal to the definition of χ_i when $f^* = 0$, except very near the equator. In the case where $f = 0$, the perturbation equation becomes

$$-\frac{\partial^6\psi}{\partial z^6} = S_i\left(\frac{\partial^2\psi}{\partial y^2} + \frac{\partial^2\psi}{\partial y\partial z}\right),$$

where

$$S_i \equiv \frac{H^4 f^{*2}\bar{U}_y^2(\sigma - 1)^2}{\nu^2[\sigma N^2 + f^*(f^* + \bar{U}_z)]}$$

and y has been scaled by

$$\frac{\sigma N^2 + f^*(f^* + \bar{U}_z)}{f^*\bar{U}_y(\sigma - 1)}H.$$

When S_i exceeds some critical value, instability will set in. The growth rate of the equatorial instability will be $O(f^{*1/2}\bar{U}_y^{1/2})$ which is somewhat slower than the usual form of inertial instability. Note also that no instability occurs when the Prandtl number is unity. Upon examination of (C8), it is evident that one must be very close to the equator before terms involving f^* become important in hydrostatic flows.

Finally, the special case of neutrally stratified flow is examined. Here we take

$$\sigma N^2 + f^*(f^* + \bar{U}_z) = 0$$

and scale both y and z by H as before. Then (C7) reduces to the form (10) with χ_{ii} redefined as

$$\chi_{ii} \equiv \frac{2f^* + (1+\sigma)\bar{U}_z}{\bar{\eta}} + \frac{f^*}{f}\frac{\bar{U}_y}{\bar{\eta}}(\sigma - 1). \quad \text{(C9)}$$

Away from the equator, the contribution of terms involving f^* is again small, since in general $\bar{U}_z \gg \bar{U}_y$ and $\bar{U}_z \gg f^*$. At the equator, the perturbation equation becomes

$$-(\nabla^2)^3\psi = S_{ii}\frac{\partial^2\psi}{\partial y\partial z},$$

where

$$S_{ii} \equiv \left|\frac{H^4 f^*\bar{U}_y(\sigma - 1)}{\nu^2}\right|.$$

Again, instability will only occur if $\sigma \neq 1$, and the growth rate will be $O(f^{*1/2}\bar{U}_y^{1/2})$.

It is evident from this analysis that the meridional component of the earth's rotation vector does not modify the inertial stability problem in any important way, even in neutrally stratified flow, except perhaps very close to the equator. In the latter case, the use of an initial state in geostrophic balance must be questionable. The smallness of the effect of the meridional component of the Coriolis terms is physically attributable to the smallness of the vertical component of shear vorticity compared to the horizontal component in most geophysical flows.

REFERENCES

Arakawa, A., and W. H. Shubert, 1974: Interaction of a cumulus cloud ensemble with the large-scale environment, Part I. *J. Atmos. Sci.*, **31**, 674–701.

Chandrasekhar, S., 1961: *Hydrodynamic and Hydromagnetic Stability*. Oxford University Press, 654 p.

Charney, J. G., and A. Eliassen, 1964: On the growth of the hurricane depression. *J. Atmos. Sci.*, **21**, 68–75.

Fritsch, J. M., C. F. Chappell and L. R. Hoxit, 1976: The use of large-scale budgets for convective parameterization. *Mon. Wea. Rev.*, **104**, 1408–1418.

Kuo, H.-L., 1954: Symmetric disturbances in a thin layer of fluid subject to a horizontal temperature gradient and rotation. *J. Meteor.*, **11**, 399–411.

McIntyre, M. E., 1970: Diffusive destabilization of the baroclinic circular vortex. *Geophy. Fluid Dyn.*, **1**, 19–58.

Pellew, A., and R. V. Southwell, 1940: On maintained convective motion in a fluid heated from below. *Proc. Roy. Soc. London.*, **A176**, 312–343.

Rayleigh, 1916: On the dynamics of revolving fluids. *Proc. Roy. Soc. London.*, **A93**, 447–453.

Solberg, H., 1933: Le mouvement d'inertie de L'atmosphére stable et son role dans la théorie des cyclones. Memoir presented to the Meteor. Assoc. U.G.G.I., Lisbon, Dupont Press, 66–82.

Stone, P. H., 1966: On non-geostrophic baroclinic stability. *J. Atmos. Sci.*, **23**, 390–400.

——, 1972: On non-geostrophic baroclinic stability, Part III. The momentum and heat transports. *J. Atmos. Sci.*, **29**, 419–426.

Walton, I. C., 1975: The viscous nonlinear symmetric baroclinic instability of a zonal shear flow. *J. Fluid Mech.*, **68**, 757–768.

Yanai, M., and T. Tokioka, 1969: Axially symmetric meridional motions in the baroclinic circular vortex: a numerical experiment. *J. Meteor. Soc. Japan*, **47**, 183–198.